A New Coordination Framework for Multi-UAV Formation Control

by

Mehmet Ali Güney

Submitted to the Graduate School of Sabancı University
in partial fulfillment of the requirements for the degree of
Master of Science

Sabancı University

July 2013

A New Coordination Framework for Multi-UAV Formation Control

APPROVED BY:

Prof. Dr. Mustafa Ünel (Thesis Advisor)	.....
Assoc. Prof. Mahmut F. Akşit	.....
Assoc. Prof. Ali Koşar	.....
Assist. Prof. Hüsnü Yenigün	.....
Assist. Prof. Hüseyin Üvet	.....

DATE OF APPROVAL: 31.../07/2013

A New Coordination Framework for Multi-UAV Formation Control

Mehmet Ali Güney

ME, Master's Thesis, 2013

Thesis Supervisor: Prof. Dr. Mustafa Ünel

Keywords: UAV, Quadrotor, Backstepping Control, Coordination, Formation Control, Virtual Structure

Abstract

Unmanned Aerial Vehicles (UAVs) have become very popular in the last few decades. Nowadays these vehicles are used for both civilian and military applications which are dull, dirty and dangerous for humans. The remarkable advances in materials, electronics, sensors, actuators and batteries enable researchers to design more durable, capable, smart and cheaper UAVs. Consequently, a significant amount of research effort has been devoted to the design of UAVs with intelligent navigation and control systems.

There are certain applications where a single UAV can not perform adequately. However, carrying out such tasks with a fleet of UAVs in some geometric pattern or formation can be more powerful and more efficient. This thesis focuses on a new coordination scheme that enables formation control of quadrotor type UAVs. Coordination of quadrotors is achieved using a virtual structure approach where orthogonal projections of quadrotors on a virtual plane are utilized to define coordination forces. This plane implies planar spring forces acting between the vehicles. Virtual springs are also augmented with dampers to suppress oscillatory motions. While the coordination among the aerial vehicles is achieved on a virtual plane, altitude control for each vehicle is designed independently. This increases maneuvering capability of each quadrotor along the vertical direction. Due to their robustness to the external disturbances such as wind gusts, integral backstepping controllers are designed to control attitude and position dynamics of individual quadrotors. Several coordinated task scenarios are presented and the performance of the proposed formation control technique is assessed by several simulations where three and five quadrotors are employed. Simulation results are quite promising.

Çoklu İnsansız Hava Aracı Oluşum Kontrolü için Yeni Bir Koordinasyon Yapısı

Mehmet Ali Güney

ME, Master Tezi, 2013

Tez Danışmanı: Prof. Dr. Mustafa Ünel

Anahtar Kelimeler: İHA, Dört-Rotor, Geri Basaklama Kontrol, Koordinasyon, Oluşum Kontrolü, Sanal Yapı

Özet

İnsansız Hava Araçları (İHA) son birkaç on yıl içinde çok popüler hale gelmişlerdir. Günümüzde bu araçlar, insanlar için sıkıcı, kirli ve tehlikeli sivil ve askeri uygulamalar için kullanılmaktadır. Malzeme, elektronik, sensör, motor ve pil alanlarındaki dikkat çekici gelişmeler daha dayanıklı, yetenekli, akıllı ve ucuz İHA'ların yapımını mümkün kılmıştır. Sonuç olarak, önemli derecede araştırma çabası akıllı navigasyon ve kontrol sistemlerine sahip İHA'ların tasarımına adanmıştır.

Tek bir İHA'nın başarılı bir şekilde yerine getiremeyeceği uygulamalar vardır. Ancak, geometrik örüntü veya oluşum halindeki bir İHA filosu bu görevleri daha güçlü ve verimli bir şekilde gerçekleştirebilir. Bu tez çalışması quadrotor tipi İHA'ların oluşum kontrolüne imkan sağlayan yeni bir oluşum kontrol şeması üzerine odaklanmıştır. Quadrotorların koordinasyonu sanal yapı yaklaşımı ile geliştirilmektedir, koordinasyon kuvvetleri quadrotorların sanal bir düzleme dikey izdüşümleri kullanılarak tanımlanmıştır. Araçlar arasında sanal düzlemde tanımlanan düzlemsel yay kuvvetleri bulunmaktadır. Bu sanal yay kuvvetleri, salınımlı hareketleri durdurması için amortisörlerle desteklenmiştir. Uçan robotların koordinasyonu düzlemsel yüzeyde başarılırken aracın yükseklik referansı koordinasyon modelinden bağımsız olarak aracın üzerinde üretilir. Bu her bir quadrotora dikey düzlemde daha fazla manevra kabiliyeti özgürlüğü eklemektedir. Quadrotorun yönelim ve pozisyon kontrolü, rüzgar gibi dış bozucu etkilere karşı gürbüz olusundan dolayı integral geribasamaklama yöntemi kullanılarak tasarlanmıştır. Çeşitli koordineli görev senaryoları sunulmuştur ve önerilen oluşum kontrol yönteminin performansı benzetim çalışmlarında üç ve beş quadrotor kullanılarak incelenmiştir. Benzetim sonuçları oldukça ümit vericidir.

Acknowledgements

I would like to express my sincere gratitude and appreciation to my thesis advisor Prof. Dr. Mustafa Ünel for his invaluable guidance, support, personal encouragements and bright insights throughout my M.S. study. I am greatly indebted to him for giving me the chance to carry out my M.S. thesis work in a motivating project environment.

I would like to thank Assoc. Prof. Mahmut F. Akşit, Assoc. Prof. Ali Koşar, Assist. Prof. Hüsnü Yenigün and Assist. Prof. Hüseyin Üvet for their feedbacks and spending their valuable time to serve as my jurors.

I would like to acknowledge the financial support provided by The Scientific & Technological Research Council of Turkey (TÜBİTAK) through BIDEB scholarship.

I would sincerely like to thank Control, Vision and Robotics Research team members Alper Yıldırım, Barış Can Üstündağ, İbrahim Taygun Kekeç pleasant team-work and efforts in UAV project. I would also like to thank Sanem Evren and Soner Ulun for their support throughout my Master thesis.

I would like to thank all Mechatronics laboratory members for their precious friendship and the great time that we spent together throughout my M.S. study.

I would like to thank by heart my girlfriend Ece Alpaslan for all her unending love, support and motivation that fed me throughout my Master thesis.

Finally, I would like to thank my entire extended family for all their love, motivation and the support throughout my life. They have always been there for me to overcome all challenges in my life.

Contents

List of Figures

List of Tables

Chapter I

1 Introduction

The robotics community has shown a growing research interest into unmanned aerial vehicles (UAVs) and micro aerial vehicles (MAVs) during the last couple of decades. Such aerial vehicles are also known as "robotic aircraft" and their uses have become more spread. An unmanned aerial vehicle is defined as an aircraft that does not carry crew, uses aerodynamic forces to provide vehicle lift, can fly autonomously or piloted remotely, can be expendable or recoverable, and carry a lethal or non-lethal payload [1].

UAVs are more suitable for dull, dirty and dangerous missions than manned aircrafts. The low downside risk and higher confidence in the operation success are main motivations for growing usage of UAVs. Therefore, technological, economic and political factors have stimulated development of UAVs [2]. First of all, the advances in materials, electronics, sensors, actuators and batteries enable researchers to design more durable, capable, smart and cheaper vehicles. Secondly, UAVs are successful when charged with mission and battlefield. Thus, they have been getting more funding and a large number of production orders. Third, UAVs can operate in dangerous and contaminated environments, and operate in other environments denied for manned aircrafts, such as altitudes that are both lower and higher than those typically traversed by manned aircraft.

According to UAV market studies, it is predicted that the worldwide UAV market will enlarge significantly in the next decade. Moreover, in these studies it also is estimated that UAV spending will be more than triple, totaling close to 55 billion in the next 10 years. U.S UAV market will reach 16 billion in the next 5-7 years, whereas Europe will spend only 3 billion [3, 4]. In Fig. 1.1, U.S UAV market development budget has started to increase rapidly after 2001, and research and development gained acceleration [1]. On the other hand, in Fig. 1.2 UAV research and development budgets in Europe has increased slowly when it is compared with U.S. UAV investment.

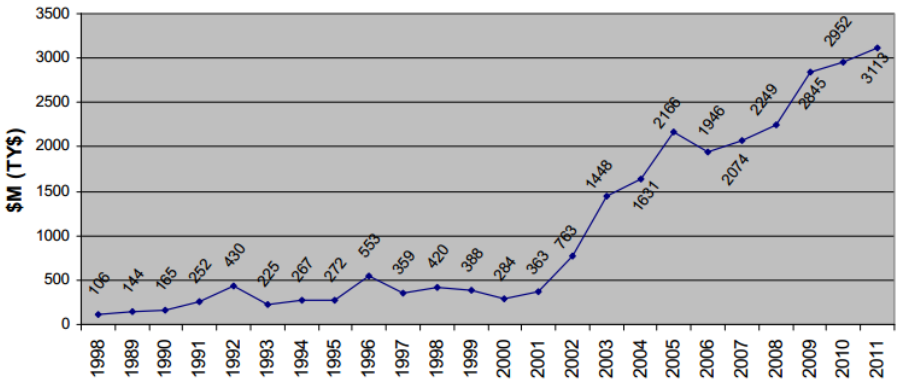

Figure 1.1: Annual funding of the U.S. Department of Defense [1]

Nowadays these vehicles are used for both civilian and military applications. The primary usage of UAV is millitary applications. Civilian usage of UAV also called commercial usage is 3% of total UAV market [5]. Moreover, civilian market is expected to grown more rapidly when it is compared with military market. In [6], it is stated that the growth in the civilian market will be four or five times faster than the military market in the next ten to twenty years.

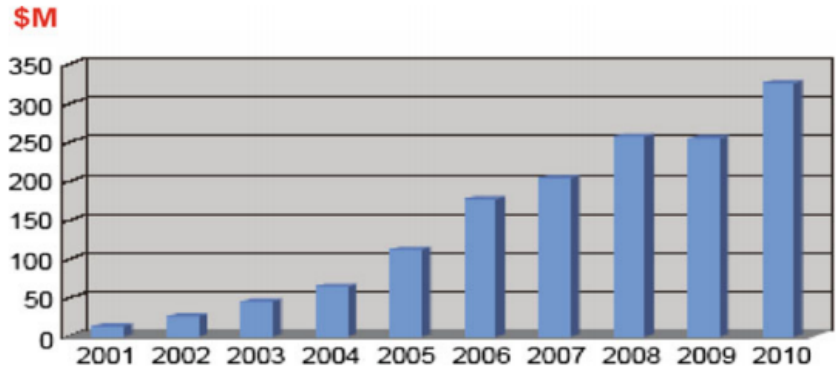

Figure 1.2: Annual funding in Europe[2]

Some significant applications of the civilian usage of the UAVs are given below [6]:

- Communication Relays (equivalent to low-altitude satellites or cell towers)
- Media (overhead cameras for news and special events)
- Surveying (city and suburban planning)
- Farming and Ranching (check on cattle, fence lines, and work crews, spraying crops with pesticide and fertilizer, monitoring crops, soil, moisture, and pest conditions, and insect sampling)
- Film Industry (aerial photography and special effects)
- Archaeology (aerial observation of sites and digs)
- Oil and Mineral Industry (gas and oil pipeline monitoring in desolate areas, search for mineral and fossil fuel deposits)

- Energy Facilities (monitoring nuclear facilities, reconnaissance for hazardous waste cleanup, atmospheric and climatic research)

Moreover, UAVs have some important military applications where they reduce the human life risks, workloads and direct enemy contact [7].

- Reconnaissance and Surveillance (wide-area search and multi-intelligence capability, ability of processing, exploitation and dissemination)
- Security (operations to preserve friendly force combat power and freedom of maneuver)
- Close Combat (operating as a part of the combined arms team when conducting decisive, integrated, air-ground operations)
- Chemical, Biological, Radiological, Nuclear and High Yield Explosives Reconnaissance (The ability to find harmful material or hazards and to survey the affected areas)
- Interdiction Attack (degrading, neutralizing, or destroying enemy combat)
- Strike (conduct high risk and high payoff attack/strike operations with minimal exposure of manned systems)
- Target Identification and Designation (identify and precisely locate military targets in real-time)
- Combat Support (distinguish between friend, enemy, neutral, and noncombatant)

- Sustainment (supply/retrograde operations, extraction of damaged parts for repair)

UAVs can also be categorized by their mechanical structures and configurations such as fixed-wing, rotary-wing and hybrid designs [2]. The oldest researches on UAVs were conducted on fixed-wing mechanism that generally refers to unmanned airplanes with wings. Fixed wing UAVs are simple to control, have long endurance and they are suited for wide area surveillance and tracking applications. Another advantage of fixed wing UAVs is that they can sense images at long distances. However they are not suitable for indoor applications due to their high speed requirement. Furthermore, they have disadvantage against rotary wing UAVs that fixed wing UAVs need space and time to regain its course [8].

On the other hand, rotary wing UAVs are called as Vertical Take-off and Landing (VTOL) UAVs. The VTOL UAVs have high maneuverability and they are able to hover at a fixed point [8]. However, rotary wing UAVs have disadvantages against fixed wing UAVs such as short endurance and low flight speed. Quadrotors are gaining increasing interest as rotary wing UAVs. This type of rotorcraft achieve flight by balancing the forces produced by four rotors. They have low cost and small size, and they become broadly available. Quadrotors are able to lift relatively high payloads and provide an increasingly broad set of basic functionalities. The drawback of this type of rotarycraft is energy consumption augmentation due to the extra motors [9–11].

Besides this conventional aerial vehicle designs, hybrid designs also exist that combine advantages of fixed-wing and rotary-wing UAVs [12, 13]. Hybrid designs can reach high speeds and they have long endurance because of

the fixed-wing structure. Moreover, they can takeoff and land vertically, a feature comes from rotary wing UAVs. Some examples of fixed wing, rotary wing and hybrid design UAVs are given in Table 1.1

Table 1.1: Examples of different types of UAVs according to their configurations

Type of UAV	Institute/Company Name	Name of UAV	
Fixed-Wing	AAI	Aerosonde [14]	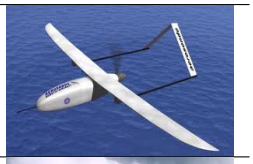
Fixed-Wing	Boeing	X-45B [15]	
Rotary-Wing	Mikrokopter	Quadro XL [16]	
Rotary-Wing	Ascending Technologies	Hummingbird III [17]	
Hybrid	Chiba University & G.H. Craft	QTW UAS-FS4 [18]	
Hybrid	Sabanci University	SUAVI [13]	

Quadrotors have nonlinear and time varying dynamics. In addition, they are under-actuated systems with four control inputs and 6 DOF pose parameters. Quadrotor models are usually subject to unmodeled dynamics,

parametric uncertainties, and they are constantly affected by aerodynamic disturbances. Thus, they require advanced control strategies to achieve good performance in piloted or autonomous flight with high maneuverability and robustness with respect to external parametric uncertainties and disturbances [11].

In the literature there are several methods to control quadrotors. In [19], LQ and classical Proportional-Integral-Derivative (PID) which are model based control approaches used to control the quadrotor. Authors showed that these two methods are able to control attitude angles of quadrotor in the presence of minor disturbance. Voos [20] divide nonlinear control system into nested control structures and design feedback linearization control approach. The decomposed system has velocity control system in the outer loop and attitude control system in the inner loop. Altug et al. utilized backstepping control method to stabilize a quadrotor by keeping the positions and the yaw angle constant and the pitch and the roll angle zero [21, 22]. In further work [23], authors improved the performance of the backstepping control by incorporating the integral action which eliminates steady state error and is robust to disturbances. In other words, they designed integral backstepping approach for attitude and position control of the quadrotor. Nicol et al. [24], proposed adaptive control strategy with Cerebellar Model Arithmetic Computer (CMAC) algorithm. CMAC algorithm provides computationally-efficient and accurate approximator that adapts quickly. The proposed method is adaptive to model uncertainties and is robust to disturbances. In [25, 26], a quadrotor is controlled by using sliding mode control. Sliding mode is insensitive to model errors, parametric uncertainties and other disturbances. In [25], authors proposed sliding mode

control method by decomposing the quadrotor system into a fully-actuated subsystem and an under-actuated subsystem. In this method, quadrotor achieve desired position with desired yaw angle by keeping roll and pitch angle around zero. In [26], Block Control Technique is combined with second order sliding mode super-twisting algorithm to design a robust flight controller. In the proposed control method, block control technique provides attitude control while sliding mode control provides longitudinal, latitudinal and heading motions where control loops are independent. In [27], the author develops a control system based on a combination of state-dependent Riccati equations and neural networks. Quadrotor control system is decomposed into a velocity control system in the outer loop and an attitude control system is in the inner loop as in [20]. The inner-loop, attitude control system, is designed using state-dependent Riccati equations, and the outer loop, the velocity control system, is designed using neural networks. Raffo et al [11], designed integral predictive and robust H_∞ control strategy to solve the path following problem of quadrotor. They proposed a hierarchical control structure. In outer loop state-space predictive controller is designed to track reference trajectory while inner loop is designed based on H_∞ controller able to reject sustained disturbances due to the use of the integral action.

Besides there are some applications, where a single quadrotor can not achieve perfectly, such as surveillance, search and rescue, law enforcement and border patrol. These applications require several robots to achieve the task in a coordinated fashion because individual vehicles can sense changes in the environment, exchange information with each other and may go into action together. Therefore, researchers developed multiple quadrotor testbeds to implement these tasks. Some of those testbeds are built at Stanford Uni-

versity, University of Pennsylvania and Swiss Federal Institute of Technology Zurich (ETH) which are also called as Stanford Testbed of Autonomous Rotorcraft for Multi-Agent Control (STARMAC), General Robotics, Automation, Sensing, and Perception (GRASP) and Flying Machine Arena (FMA), respectively. STARMAC testbed [28–31] is outdoor quadrotor testbed for testing and validating multi-agent algorithms and control schemes by using Draganflyer quadrotors. Since it is an outdoor testbed quadrotors are equipped with GPS, IMU and ultrasonic sensors to obtain the pose of quadrotor. They performed autonomous hover and outdoor autonomous trajectory tracking with quadrotors. GRASP testbed [32–36], support research on coordinated motion of (MAVs) with broad applications such as reconnaissance, surveillance, manipulation and transport. These applications are performed by Ascending technologies Hummingbird quadrotor. The pose of quadrotors are provided by Vicon motion capture system with $50\mu m$ accuracy. The main research focus is developing new control algorithm for MAVs and coordination actions with multiple MAVs. Flying Machine Arena [37–40], uses modified Ascending Technologies Hummingbird quadrotors and they have 10 $\times$ 10 $\times$ 10 m^3 space enclosed by nets on the sides and pads are placed on the floor. The space is equipped with Vicon motion capture system for getting the pose of the quadrotors with millimeter accuracy. Lots of application are achieved such as balancing an inverted pendulum, juggling balls, flipping and constructing 6 m structure consisting of 1500 foam bricks.

1.1 Thesis Organization and Contributions

In Chapter II, background information on multi agent coordination and formation control is given and various types of formation structures are de-

scribed.

In Chapter III, a nonlinear dynamic model of a quadrotor is obtained using Newton-Euler method. Backstepping controllers are designed to control quadrotor's attitude and position dynamics.

In Chapter IV, a new coordination framework along with a virtual reference model is presented. In the proposed scheme, quadrotors are modeled as point masses and they are connected with virtual springs and dampers. Moreover, quadrotors are attracted to the target via spring and damper forces. Spring coefficients are modeled as an adaptable parameter to reach a uniform circular formation around the target at a certain distance.

Chapter V focuses on the simulations results of the proposed formation control technique. The performance of the proposed formation method is assessed by using three and five quadrotors in the group.

Chapter VI concludes the thesis work and indicates possible future directions.

Contributions of the thesis can be summarized as follows:

- A nonlinear dynamic model of a quadrotor is derived using Newton-Euler method.
- Attitude and position controllers for a quadrotor are designed using integral backstepping control approach.
- A planar virtual reference model, which is composed of point masses connected via springs and dampers, is proposed to generate reference trajectories for each aerial vehicle in the group.
- Uniform distribution of quadrotors around the target is achieved by switching the adaptable spring coefficients.

1.2 Notes

The following papers are produced from the thesis work:

- Quadrotorlar için İleri Besleme Terimi Frenet-Serret Teorisiyle Hesaplanan İntegral Geri Basamaklama Denetleyicisinin Performans Analizi, M. A. Güney, M. Ünel, TOK'12: Otomatik Kontrol Ulusal Toplantısı. October 11-13, 2012.

- Formation Control of a Group of Micro Aerial Vehicles (MAVs), M. A. Güney, M. Unel, IEEE International Conference on Systems, Man, and Cybernetics (SMC 2013), October 13-16, 2013.

- A Modular Software Architecture for UAVs, T. Kekec, B. C. Ustundag, M. A. Güney, A. Yildirim, M. Unel, 39th Annual Conference of the IEEE Industrial Electronics Society (IECON 2013), November 11-13, 2013.

- İnsansız Hava Araçları için Donanımdan Bağımsız Yazılım Sistemi Geliştirilmesi, B. C. Ustundag, T. Kekec, M. A. Güney, P. Mundt, M. Unel, TOK'13: Otomatik Kontrol Ulusal Toplantısı, September 26-28, 2013 (Submitted).

1.3 Nomenclature

Symbol	Description
c_1	convergence speed of the roll angle loop
c_2	convergence speed of the roll angular speed loop
c_3	convergence speed of the pitch angle loop
c_4	convergence speed of the pitch angular speed loop
c_5	convergence speed of the yaw angle
c_6	convergence speed of the yaw angular speed loop
c_7	convergence speed of the x position loop
c_8	convergence speed of the y position loop
c_9	convergence speed of the z position loop
c_{10}	convergence speed of the x linear speed loop
c_{11}	convergence speed of the y linear speed loop
c_{12}	convergence speed of the z linear speed loop
c_{coord}	coordination force damper coefficient
c_{targ}	target force damper coefficient
d	motor drag coefficient
d_{break}	distance to be preserved among the virtual masses
d_{coord}	coordination distance to be preserved among the virtual masses
d_{i2j}	signed distance between m_i and m_j
d_{i2T}	signed distance between m_i and target
d_{target}	distance to be preserved among the virtual masses and target
d_{near}	distance to be preserved among the virtual masses in the second stage
e_1	roll tracking error
e_2	roll angular speed tracking error
e_3	pitch tracking error
e_4	pitch angular speed tracking error
e_5	yaw tracking error
e_6	yaw angular speed tracking error

Symbol	Description
e_7	x position tracking error
e_8	y position tracking error
e_9	z position tracking error
e_{10}	x linear speed tracking error
e_{11}	y linear speed tracking error
e_{12}	z linear speed tracking error
$E(\phi, \theta)$	rotational velocity transformation matrix
F_{aero}	aerodynamic forces generated by the wings
F_{coord}	coordination force between the quadrotors
F_g	gravity force
F_i	thrust force of each rotor
F_m	thrust force created by rotors
F_t	total external force acting on the quadrotor
F_{targ}	target force between quadrotor and the target
g	gravity
I	inertia matrix of the quadrotor in body frame
I_{xx}	moment of inertia around x_b in body frame
I_{yy}	moment of inertia around y_b in body frame
I_{zz}	moment of inertia around z_b in body frame
J_{prop}	inertia of the propellers about their rotation axis
k	motor lift coefficient
k_{coord}	coordination force spring coefficient
k_{far}	coordination force spring coefficient in the first stage
k_{near}	coordination force spring coefficient in the second stage
k_{targ}	target force spring coefficient
l	distance between rotor and center of gravity
m	mass of the quadrotor
M_{aero}	aerodynamic moment due to lift/drag forces
M_g	gyroscopic moments
M_i	rotor moments

Symbol	Description
M_t	total moments acting on the quadrotor
n_{i2j}	unit vector from m_i to m_j
n_{i2T}	unit vector from m_i to target
O_b	origin of body frame
O_e	origin of earth frame
p	angular velocity of the aerial vehicle about x_b in body frame
P_e	position of the quadrotor in earth frame
q	angular velocity of the aerial vehicle about y_b in body frame
Q_i	each quadrotor in the group
r	angular velocity of the aerial vehicle about z_b in body frame
$R(\phi, \theta, \psi)$	orientation of world frame wrt. the earth frame
T	target for a group of quadrotor
U_1	total thrust
U_2	rolling moment
U_3	pitching moment
U_4	yawing moment
V_e	linear velocity of the quadrotor in earth frame
V_b	linear velocity of the quadrotor in body frame
V_x	linear velocity along x_b in body frame
V_y	linear velocity along y_b in body frame
V_z	linear velocity along z_b in body frame
x	position of the aerial vehicle along x_e in earth frame
x_b	x axis of body frame
x_d	desired position of the aerial vehicle along x_e in earth frame
x_e	x axis of earth frame
$\dot{X}_i$	velocity vector of m_i
$\dot{X}_j$	velocity vector of m_j
$\dot{X}_k$	velocity vector of m_k
y	position of the aerial vehicle along y_e in earth frame
y_b	y axis of body frame

Symbol	Description
y_d	desired position of the aerial vehicle along y_e in inertial frame
y_e	y axis of earth frame
z	position of the aerial vehicle along z_e in earth frame
z_b	z axis of body frame
z_d	desired position of the aerial vehicle along z_e in inertial frame
z_e	z axis of earth frame
α_e	attitude of the quadrotor in earth frame
χ_1	integral of roll tracking error
χ_2	integral of pitch tracking error
χ_3	integral of yaw tracking error
χ_4	integral of x position tracking error
χ_5	integral of y position tracking error
χ_6	integral of z position tracking error
ω_i	propellers rotational speed
ω_x	roll angular speed
ω_x^d	desired roll angular speed
Ω_x	angular velocity of the quadrotor in earth frame
Ω_b	angular velocity of the quadrotor in body frame
Ω_e	angular velocity of the quadrotor in earth frame
θ	pitch angle, angular position around y_w
θ_d	desired pitch angle
ϕ	roll angle, angular position around x_w
ϕ_d	desired roll angle
ψ	yaw angle, angular position around z_w
ψ_d	desired yaw angle
μ_1	virtual control input for x axis
μ_2	virtual control input for y axis
μ_3	virtual control input for z axis

Chapter II

2 Background on Multi Agent Coordination

Robotic vehicles that move in a formation can carry out certain tasks that can not be performed by a single vehicle. Applications of vehicle formation control include coordination and cooperation of unmanned ground vehicles(UGVs), unmanned air vehicles(UAVs), autonomous underwater vehicles(AUVs). In the literature there are several approaches to the group coordination problem such as behavior based, leader follower, virtual structure and graph theory.

The advantage of the behavioral approach is that it is natural to develop control approach when agents have multiple competing objectives. In addition, each agent has feedback information which means each agent reacts according to the position of its neighbors. Another advantage of behavioral approach is that it permits itself naturally to a decentralized formation control implementation. The disadvantage of behavior approach is that the group behavior can not be defined explicitly. In addition, it is difficult to analyze the behavioral approach mathematically and guarantee its group stability [41]. An important advantage of the leader follower control scheme is its mathematical simplicity. However, the major disadvantage of the leader-follower approach is the leader which is the single point of failure of the

formation, namely if something wrong happens to the leader, then the formation mission can not be achieved. The advantage of the virtual structure approach is that it is easy to define the formation behavior for the group. Another advantage is that the virtual structure can maintain the formation very well during the maneuvers, namely, the virtual structure can evolve as a whole in a given direction with some given orientation and maintain a rigid geometric relationship among multiple vehicles. The disadvantage is that requiring the formation to act as a virtual structure limits the class of potential applications of this approach [42]. Convenience of these approaches are highly application specific.

2.1 Behavior Based Formation Control

Behavior-based robotics is inspired from intelligent behaviors of animals. A behavior is a mapping of function producing responses from stimuli [43]. Behavior based control is a decentralized control strategy used to autonomously control one robot or a group of robots. Note that a decentralized control system for an individual robot means that there is no planning or reasoning for the generation of responses. However, a decentralized or distributed control systems for multi robots indicates that there is no control part managing the system.

In behavior based formation control approach exact models are not necessary. The task is decomposed into object-oriented behaviors, which requires to accomplish its objective. Each behavior is independent and can have direct access to the sensors and actuators of the robot. Behavioral control is decomposed into subproblems which are behaviors or tasks. Monteiro and Bicho [44], propose behavior-based formation control by using nonlinear dy-

namical systems. The authors utilize three autonomous mobile robots which do not have prior knowledge about the environment to navigate in triangle formation, and avoid obstacles in the environment. Liu and Shi [45], introduce behavior-based formation control for mobile robots. They use dynamic dead zone method to maintain the planned formation. Moreover, they utilize combination of potential function based avoidance and wall following behavior to guarantee obstacle avoidance.

In [46], a behavior-based formation control of MAV is introduced to generate the formation flight control command in terms of accelerations. The hierarchy in the group is provided by the leader follower method to form a structure of the group. Sentang et al. [47], propose behavior-based high dynamic autonomous formation and control method for multi-missile system that combine the behavior based control with the leader follower method. Authors use the advantages of the conventional behavior based method which are parallelism, distributing and real-time. On the other hand, they cover the disadvantages of the behavior-based control, realizing the unification of the autonomy and community of multi-missile by using leader follower method.

In [48], the formation control problem of multiple autonomous underwater vehicles (AUV) is investigated. Authors propose a new control algorithm based on potential function and behavior rules to effectively control the formation of the multiple AUV in certain environment and make the formation effectively avoid obstacles. In [49, 50], Null-Space based behavioral control is presented mobile robots and marine surface vessels. In [50], authors propose a new task function to be used by the Null Space based behavior control method to obtain a predefined mobile robot formation. Furthermore in [49], Null Space based behavior control is considered as a high level controller that

selects the motion references for each vessel of the fleet. The method guides the fleet in the complex environment, and at the same time it can achieve multiple tasks such as obstacle avoidance and keeping the formation.

2.2 Leader Follower Formation Control

In leader follower based control some of the agents are designated as leaders. These leaders can transmit location and orientation information to other agents. However, leader does not receive any information from other agents. On the other hand, some of the agents which are designed as followers can transmit and receive information [51].

Ramirez and Linares [52], designed a linear robust dynamic output feedback control scheme for output reference trajectory tracking tasks by using leader follower formation approach for non-holonomic mobile robots. In this method, the follower robot knows only the position of the leader, but delay is included in communication among the robots. Moreover, unknown disturbances are modelled as absolutely bounded, additive and unknown signals. Futhermore, they designed a linear Luenberger observer to estimate disturbance, and disturbance is eliminated by the local follower's controller actions via online cancellation effort. Saad et al. [53], investigate the leader follower motion coordination of non holonomic mobile robots which combine virtual vehicle and trajectory tracking approach. They considered that the required informations from the leader are positions and heading. In addition, they designed an observer to estimate the velocity of the leader. Backstepping based control law is proposed for followers to track the reference trajectories. Furthermore, they utilize fuzzy logic approach to avoid obstacles and other follower robots. Yan et al [54], introduce adaptive formation control method

for a group of mobile robots. In this method, there are two leader robots which sense only the relative position of each other. Moreover, the followers which could be extended to n robots has two neighbor robots and each follower measure neighbors position in its coordinate system. Furthermore, according to proposed adaptive scheme, the follower robot utilizes the measured relative position information to form desired triangular formation with its two leading neighbors. The proposed adaptive scheme reduces the cost of broadcasting the velocity information and it assures that the robots can be adaptively recovered to the desired formation in the presence of an abrupt change of reference velocity. Tosques et al. [55], propose leader follower formation control method for mobile robots that keeps two variables constant, a distance and an angle. They use the angle which is referred to the follower and not to the leader. This allows the use of decentralized sensing system that guarantees approaching a higher degree of distribution. In [56], vision based formation control of mobile robots is investigated by using leader follower approach. The proposed method, utilizes the vision based algorithm to estimate the relative pose of the leader in the camera field of view given in a single known length. The relative velocity of the leader is estimated by using the nonlinear estimator. In addition, the proposed decentralized controller uses relative image information instead of position and velocity of the leader in the global reference frame. This provides elimination of the need for a communication among the agents.

In [57], Choo et al. propose leader follower formation control approach for AUV in the horizontal plane. In this method, less information is expected to be shared when compared to land and air robots, because communication is weak under water due to low bandwidth and low update rates. As a result

of that, the follower acquires the leader position measurement to track the reference trajectory in accordance with predefined distance without information on leader velocity and dynamics. Furthermore, tracking controller is designed via Lyapunov analysis and backstepping method for follower robot to enable tracking the leader robot.

In [58], Ozbay et al. focus on designing decentralized control architecture, distributed among each autonomous agent, to control a leader-follower formation of terrestrial UAVs. Each vehicle is controlled utilizing only information between its motion relative to a designated leader. In addition, they use inertial model paradigm to handle uncertainties on the leader reference trajectory and parameter uncertainties on the plant model. In [59], Dierks and Jagannathan propose leader follower formation method for quadrotors UAVs. This method based on spherical coordinates and the desired position of the follower quadrotor is designed using the desired seperation, the angle of incidence and the bearing. In addition, a new control law is derived using neural networks to learn the complete dynamics of the quadrotor online, including unmodeled dynamics like aerodynamic friction and in the presence of bounded disturbances.

2.3 Virtual Structure Formation Control

In the virtual structure approach, the entire formation is treated as a rigid body. The positions of the vehicles in the structure are usually defined in a frame with respect to a reference point in the structure. Since a trajectory is given for the reference point, the desired position for each vehicle can be calculated as the virtual structure evolves in time [60].

In [61], Yuan and Tang introduce hierarchical virtual structure forma-

tion method for autonomous mobile robots. Mobile robots are decomposed into some clusters according to their distributions in space. Furthermore, the motion of every cluster (virtual structure) is transformed into reference trajectory of every robot. Mobile robots among and within clusters are both controlled by finite control law based on variable structure. In [62], authors propose controlling the movement of robot formations by considering both kinematic and dynamic constraints for mobile robots. Moreover, mobile robots navigate in realistic scenarios with obstacles, where formations have to comply with the environment shape, while maintaining the formation topology. This method takes into account communication issues in the mobile ad-hoc network formed by the robot team. They use the real time protocol over wireless ad-hoc networks for data interchange in cooperative control. In [63], Nijmeijer et al. design virtual structure controller for formation control of unicycle mobile robots. They proposed to use mutual coupling between the individual robots, because using mutual coupling make formation more robust against perturbations as compared to leader follower approach. In further work, they propose two distributed virtual structure formation method. In these methods, all robots plan their action based upon local interaction between neighboring robots. Moreover, they prove the global stability of the previous work.

In [42], Ren and Beard propose formation control ideas using virtual structure method for multiple spacecraft. In this work, they show the advantages of introducing formation feedback from spacecraft to the formation. The system can achieve a good performance in improving convergence speed and decreasing maneuver errors. Formation feedback provides robustness to the whole system. Moreover, formation feedback improves the robustness

with respect to choosing gains for different aircrafts. In [64], authors introduce a virtual structure formation and 3D formation tracking approaches. This method allows UAVs to track desired formation which can move slower than the UAVs minimum speed. In addition, deconfliction control is utilized to keep UAVs from colliding with one another when formation change occur. Since the fixed-wing UAVs have relatively large forward velocities the deconfliction control restrict their states and make them maneuver in 3D. Linorman and Li [65], tailor synchronization technology which synchronize the relative position tracking motion between multiple aircrafts to virtual structure approach for enhancing the performance of formation control. In [66], author introduces formation control scheme which integrates dynamic formation reference generator and an extended trajectory tracking control method for fixed-wing UAVs. The proposed method allows the fixed-wing UAV to execute dynamic formation changing maneuvers based on planned relative curvilinear trajectory of each UAV in the formation. Direct trajectory generation strategy includes computing reference trajectory for each UAV to be executed in real time and enabling the relative curvilinear trajectories to be expressed directly. These two features allow formation of fixed-wing UAVs to response to a new desired formation plan rapidly. Low and San [67], propose virtual structure formation control method which allow fixed-wing UAVs to smooth formation turning along a planned formation trajectory by relaxing the rigid separation constraint between vehicles.

2.4 Graph Theory

One of the biggest problems in the formation control is the sensor information which means each robot must have information about its neighbors. A

graph theory is particularly useful and commonly used way to encode this information [68].

Dong and Farrell [69], discuss the cooperative control of mobile robots with a given formation and a desired trajectory as a group. They proposed unified error which consists of formation and tracking errors. Graph theory and Lyapunov theory are used to design control laws. In further work [70], they consider two formation control problems for mobile agents. In the first problem, they discuss formation control law where all mobile agents converge to the same stationary point with different communication scenarios. In the second problem, they discuss a formation control law where a group of mobile agents converges to and tracks a target point which moves along a desired trajectory with different communication scenarios. Cooperation control laws in this work are proposed with the aid of suitable transformations and results from graph theory.

In [71], each robot in the formation is a node of a graph where application of graph theory to formation control of UAVs with linear dynamics was introduced. Moreover the aim is to achieve development of information exchange strategies that have direct role on improvement of performance and stability and robustness to variations in communication topology.

Azuma and Karube [72], propose a formation control method with fault-tolerance. In this approach, they achieve formation control with fault tolerance by using rigidity in the graph theory with virtual structure. An optimization framework for target tracking with a group of mobile robot is presented in [73]. Authors modeled target tracking problem as a generic semidefinite program(SDP). Their methodology is based on graph theoretic results where the second smallest eigenvalue of the interconnection graph

Laplacian matrix is a measure for the connectivity of the graph. Agent target coverage and inter-agent communication constraints are modeled as linear-matrix inequalities with the help of this method. Pappas et al. [74], introduce a theoretical framework for controlling graph connectivity in a mobile robot network. The proposed method is based on combination of a variety of mathematical tools. These tools are ranging from spectral graph theory and semi-definite programming to maximize the algebraic connectivity of a network, to gradient-descent algorithms and hybrid systems to ensure topology control in a least restrictive manner. In [75], decentralized formation approach is proposed to increase the connectivity of the formation system. The connectivity of the multi-agent system is appraised through the second smallest eigenvalue of the state dependent Laplacian of the proximity graph of the agent. In this method, a supergradient algorithm is used in conjunction with decentralized algorithm for eigenvector computation to maximize the second smallest eigenvalue of the Laplacian of the proximity graph. Ford et al. [76], claim that state of the art formation schemes are limited by a high communication load, high energy consumption and lack of robustness. These areas on formation control should be improved. They introduced formation structure which reduces computational effort by using graph theory and minimal constraint to enable formation control without the need for inter robot communication, thus reducing energy consumption.

Chapter III

3 Quadrotor Modeling and Control

In order to perform coordinated motion of quadrotors, in simulation a dynamical model of the quadrotor is required. The model of dynamic equations describing the attitude and position of the quadrotor are basically those of a rotating rigid body with six degrees of freedom and four inputs.

3.1 Quadrotor Model

Before modeling quadrotor dynamics we should first define coordinate systems. Position dynamics of quadrotor is expressed wrt. fixed earth coordinate frame and the rotational dynamics wrt. body fixed frame attached to the vehicle.

- Earth frame E : (O_e, x_e, y_e, z_e)
- Body frame B : (O_b, x_b, y_b, z_b)

The Earth frame which is right handed orthogonal axis system and defined by x_e, y_e, z_e. x_e is directed eastwards, y_e is directed northwards, z_e is directed upwards and O_e is the origin of the earth frame. The body frame is attached to quadrotor's center of gravity and defined by x_b, y_b, z_b (Fig. 3.1). Similarly, in the body frame, x_b is directed to the front of the vehicle, y_b is directed to the right of the vehicle, z_b is directed upwards and O_b is the origin on the

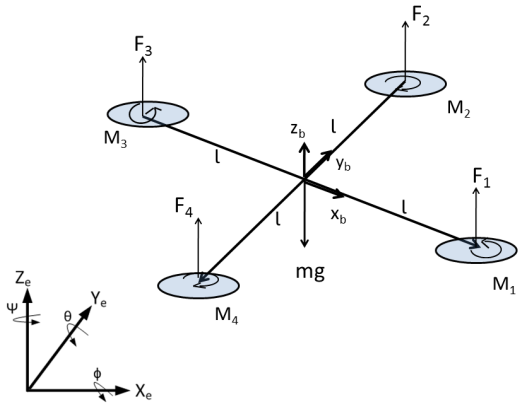

Figure 3.1: Coordinate systems and forces/moments acting on a quadrotor frame.

center of mass of the aerial vehicle. The rotors 1-4 are mounted to body on $+x_b$, $+y_b$, $-x_b$ and $-y_b$ axes, respectively.

The position and linear velocity of the vehicle's center of mass in the world frame are expressed as:

$$P_e = \begin{bmatrix} X \\ Y \\ Z \end{bmatrix} \quad , \quad V_e = \begin{bmatrix} \dot{X} \\ \dot{Y} \\ \dot{Z} \end{bmatrix} \tag{3.1}$$

Quadrotor's attitude and attitude angles' time derivative in the earth frame are defined as:

$$\alpha_e = \begin{bmatrix} \phi \\ \theta \\ \psi \end{bmatrix} \quad , \quad \Omega_e = \dot{\alpha}_e = \begin{bmatrix} \dot{\phi} \\ \dot{\theta} \\ \dot{\psi} \end{bmatrix} \tag{3.2}$$

where ϕ, θ, ψ are roll, pitch and yaw angles respectively. The orientation of the body frame with respect to the earth frame is expressed by the rotation matrix [13]:

$$R(\phi,\theta,\psi) = R_z(\psi)R_y(\theta)R_x(\phi) = \begin{bmatrix} c\psi c\theta & c\psi s\phi s\theta - c\phi s\psi & c\phi c\psi s\theta + s\phi s\psi \\ c\theta s\psi & c\phi c\psi + s\phi s\psi s\theta & c\phi s\psi s\theta - c\psi s\phi \\ -s\theta & c\theta s\phi & c\phi c\theta \end{bmatrix} \tag{3.3}$$

where cα and sα denotes $\cos(\alpha)$ and $\sin(\alpha)$, respectively. The transformation of linear velocities between the earth and the body frames is given as:

$$V_b = \begin{bmatrix} V_x \\ V_y \\ V_z \end{bmatrix} = R^T V_e \tag{3.4}$$

The relation between the angular velocity of the vehicle and time derivative of the Euler angles is given by the following transformation:

$$\Omega_b = \begin{bmatrix} p \\ q \\ r \end{bmatrix} = E(\phi,\theta).\Omega_e \tag{3.5}$$

where E is the velocity transformation matrix and defined as

$$E(\phi,\theta) = \begin{bmatrix} 1 & 0 & -s\theta \\ 0 & c\phi & s\phi c\theta \\ 0 & -s\phi & c\phi c\theta \end{bmatrix} \tag{3.6}$$

The dynamics of the unmanned aerial vehicle can be written as

$$\begin{aligned} F_t &= m\dot{V}_e \\ M_t &= I\dot{\omega} + \omega \times I\omega \end{aligned} \tag{3.7}$$

where m denotes the mass and I denotes the inertia matrix of the quadrotor. The total external forces acting on the quadrotor are motor thrusts F_i, aerodynamic forces F_{aero} and gravity force F_g. Note that position dynamics is expressed in the earth frame whereas attitude dynamics in the body fixed frame. Forces in the body frame can be transformed as follows:

$$F_t = R(F_m + F_{aero} + F_g) \tag{3.8}$$

where

$$F_m = \begin{bmatrix} 0 \\ 0 \\ \sum F_i \end{bmatrix} \quad , \quad F_g = \begin{bmatrix} mgs\theta \\ -mgc\theta s\phi \\ -mgc\phi c\theta \end{bmatrix} \tag{3.9}$$

The gravitational force is in the -z_e direction and the motor thrust forces, F_i, are in the z_b direction. Propeller thrusts $F_{(1,2,3,4)}$ are modeled as:

$$F_i = k\omega_i^2 \tag{3.10}$$

where ω_i is the motor rotational speed.

Moreover, total moment acting on a quadrotor are motor moments M_i, aerodynamic moments M_{aero} and gyroscopic moments M_g; i.e.

$$M_t = \sum M_i + M_{aero} + M_g \tag{3.11}$$

Finally, the equations of motion derived from the dynamic model are given as [13]:

$$\ddot{x} = (cos\phi sin\theta cos\psi + sin\phi sin\psi)\frac{1}{m}U_1 \tag{3.12}$$

$$\ddot{y} = (cos\phi sin\theta sin\psi - sin\phi cos\psi)\frac{1}{m}U_1 \tag{3.13}$$

$$\ddot{z} = (cos\phi cos\theta)\frac{1}{m}U_1 - g \tag{3.14}$$

$$\dot{p} = \frac{I_{yy} - I_{zz}}{I_{xx}}qr + \frac{J_p}{I_{xx}}q\Omega + \frac{U_2}{I_{xx}} \tag{3.15}$$

$$\dot{q} = \frac{I_{zz} - I_{xx}}{I_{yy}}pr + \frac{J_p}{I_{yy}}p\Omega + \frac{U_3}{I_{yy}} \tag{3.16}$$

$$\dot{r} = \frac{I_{xx} - I_{yy}}{I_{zz}}pq + \frac{U_4}{I_{zz}} \tag{3.17}$$

where U_1, U_2, U_3, U_4 are control inputs of the quadrotor and J_p is the polar moment of inertia of the propellers around the rotation axis. The control inputs are given as follows:

$$\begin{cases} U_1 = k(\omega_1^2 + \omega_2^2 + \omega_3^2 + \omega_4^2) \\ U_2 = kl(\omega_2^2 - \omega_4^2) \\ U_3 = kl(\omega_3^2 - \omega_1^2) \\ U_4 = d(\omega_1^2 - \omega_2^2 + \omega_3^2 - \omega_4^2) \\ \Omega = -\omega_1 + \omega_2 - \omega_3 + \omega_4 \end{cases}$$

where k is the thrust coefficient and d is the drag coefficient. The transformation matrix defined by Eq. (3.6) is the identity matrix at hover conditions, i.e. $\phi = \theta = 0$. It follows that around hover conditions, we have $\dot{p} \approx \ddot{\phi}$, $\dot{q} \approx \ddot{\theta}$

and $\dot{r} \approx \ddot{\psi}$. As a result, attitude dynamics can be rewritten as

$$\ddot{\phi} = \frac{I_{yy} - I_{zz}}{I_{xx}}\dot{\theta}\dot{\psi} + \frac{J_p}{I_{xx}}\dot{\theta}\Omega + \frac{U_2}{I_{xx}} \tag{3.18}$$

$$\ddot{\theta} = \frac{I_{zz} - I_{xx}}{I_{yy}}\dot{\phi}\dot{\psi} + \frac{J_p}{I_{yy}}\dot{\phi}\Omega + \frac{U_3}{I_{yy}} \tag{3.19}$$

$$\ddot{\psi} = \frac{I_{xx} - I_{yy}}{I_{zz}}\dot{\phi}\dot{\theta} + \frac{U_4}{I_{zz}} \tag{3.20}$$

3.2 Quadrotor Control System Design

Flight controller is divided into two parts which are attitude and position controllers (Fig. 3.2). Attitude control is the heart of the quadrotor control system, because it keeps quadrotor at desired orientations in three dimensions. Attitude dynamics of the quadrotor is faster than the position dynamics, so position controller is used to generate reference angles for attitude controller.

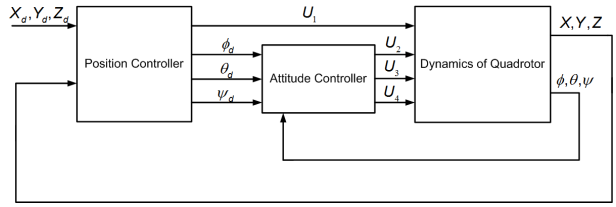

Figure 3.2: Attitude and Position Control of Quadrotor

3.2.1 Attitude Control

Attitude controller is designed using Integral Backstepping control method. This control method is chosen because it is robust to disturbances and some model uncertainties. In addition, this method guarantees asymptotic stabil-

ity, while the integral action eliminates the steady state errors. Moreover, backstepping controller design process is straightforward. The first step in integral backstepping control design is to define position tracking error $e_1 = \phi_d - \phi$ and its dynamics:

$$\frac{de_1}{dt} = \dot{\phi}_d - \dot{\phi} = \dot{\phi}_d - \omega_x \tag{3.21}$$

The angular speed ω_x is not our control input and has its own dynamics. It is set to a desired behavior and it is considered as virtual control:

$$\omega_x^d = c_1 e_1 + \dot{\phi}_d + \lambda_1 \chi_1 \tag{3.22}$$

where c_1 and λ_1 are positive constants and $\chi_1 = \int_0^t e_1(\tau) d_T$ is the integral of roll tracking error. Since ω_x has its own error e_2, its dynamics is computed using (3.22) as follows:

$$\frac{de_2}{dt} = c_1(\dot{\phi}_d - \omega_x) + \ddot{\phi}_d + \lambda_1 e_1 - \ddot{\phi} \tag{3.23}$$

where e_2, the angular velocity tracking error is defined by:

$$e_2 = \omega_x^d - \omega_x \tag{3.24}$$

Using (3.22) and (3.24) roll tracking error dynamics is rewritten as:

$$\frac{de_1}{dt} = e_2 - c_1 e_1 - \lambda_1 \chi_1 \tag{3.25}$$

By replacing $\ddot{\phi}$ in (3.23) by its corresponding expression from derived quadrotor model (3.18), the control input U_2 appears in (3.26):

$$\frac{de_2}{dt} = c_1(\dot{\phi}_d - \omega_x) + \ddot{\phi}_d + \lambda_1 e_1 - \frac{I_{yy} - I_{zz}}{I_{xx}}\dot{\theta}\dot{\psi} - \frac{J_p}{I_{xx}}\dot{\theta}\Omega - \frac{U_2}{I_{xx}} \tag{3.26}$$

The real control input now appeares in (3.26). So, using equations (3.21), (3.25) and (3.26) position tracking error e_1, angular speed tracking error e_2 and integral of the position tracking error χ_1 are combined to obtain:

$$\frac{de_2}{dt} = c_1(-c_1 e_1 - \lambda_1 \chi_1 + e_2) + \ddot{\phi}_d + \lambda_1 e_1 - \frac{\tau_x}{I_{xx}} \tag{3.27}$$

where τ_x is the overall rolling torque. The desirable dynamics for the angular speed tracking error is:

$$\frac{de_2}{dt} = -c_2 e_2 - e_1 \tag{3.28}$$

This is obtained if control input U_2 is chosen as:

$$\begin{aligned} U_2 = I_{xx}[&(1 - c_1^2 + \lambda_1)e_1 + (c_1 + c_2)e_2 - c_1\lambda_1\chi_1 + \ddot{\phi}_d \ldots \\ &- \frac{I_{yy} - I_{zz}}{I_{xx}}\dot{\theta}\dot{\psi} - \frac{J_p}{I_{xx}}\dot{\theta}\Omega] \end{aligned} \tag{3.29}$$

where c_2 is a positive constant which determines the convergence speed of the angular speed loop. Similarly, pitch and yaw control inputs are[23]:

$$\begin{aligned} U_3 = I_{yy}[&(1 - c_3^2 + \lambda_2)e_3 + (c_3 + c_4)e_4 - c_3\lambda_2\chi_2 + \ddot{\theta}_d \ldots \\ &- \frac{I_{zz} - I_{xx}}{I_{yy}}\dot{\phi}\dot{\psi} - \frac{J_p}{I_{yy}}\dot{\phi}\Omega] \end{aligned} \tag{3.30}$$

$$U_4 = I_{zz}[(1 - c_5^2 + \lambda_3)e_5 + (c_5 + c_6)e_6 - c_5\lambda_3\chi_3 + \ddot{\psi}_d \ldots - \frac{I_{xx} - I_{yy}}{I_{zz}}\dot{\phi}\dot{\theta}] \tag{3.31}$$

where c_2, c_3, c_4, c_5, c_6, λ_2, λ_3 are positive constants and χ_2, χ_3 the integral position tracking error of pitch and yaw angles, respectively.

3.2.2 Position Control

Position controller ensures to keep the quadrotor at a desired position. Vertical motion is provided by motor thrusts, but horizontal motion is provided by changing the thrust vector direction into desired motion direction. The motion on X and Y directions can be achieved by rolling and pitching quadrotor respectively. The outputs of the position controller are reference roll angle, ϕ_d, reference pitch, θ_d and the total thrust, U_1. Since both vertical and horizontal motion depend on thrust vector, virtual control inputs are designed as Integral Backstepping controller for achieving the position control [2, 13]

In order to design position controller, first the quadrotor position (X, Y, Z) dynamics is recalled; i.e

$$\ddot{x} = (cos\phi sin\theta cos\psi + sin\phi sin\psi)\frac{1}{m}U_1 \tag{3.32}$$

$$\ddot{y} = (cos\phi sin\theta sin\psi - sin\phi cos\psi)\frac{1}{m}U_1 \tag{3.33}$$

$$\ddot{z} = (cos\phi cos\theta)\frac{1}{m}U_1 - g \tag{3.34}$$

We define position tracking errors as follows:

$$\begin{cases} e_7 = x_d - x \\ e_8 = y_d - y \\ e_9 = z_d - z \end{cases} \tag{3.35}$$

Similarly angular speed tracking error is defined as:

$$\begin{cases} e_{10} = c_7 e_7 + \dot{x}_d + \lambda_4 \chi_4 - \dot{x} \\ e_{11} = c_8 e_8 + \dot{y}_d + \lambda_5 \chi_5 - \dot{y} \\ e_{12} = c_9 e_9 + \dot{z}_d + \lambda_6 \chi_6 - \dot{z} \end{cases} \tag{3.36}$$

Virtual control inputs μ_{1-3} are given as follows [23]:

$$\mu_x = \ddot{x}_d + (1 - c_7^2 + \lambda_4)e_7 + (c_7 + c_{10})e_{10} - c_7 \lambda_4 \chi_4 \tag{3.37}$$

$$\mu_y = \ddot{y}_d + (1 - c_8^2 + \lambda_5)e_8 + (c_8 + c_{11})e_{11} - c_8 \lambda_5 \chi_5 \tag{3.38}$$

$$\mu_z = \ddot{z}_d + (1 - c_9^2 + \lambda_6)e_9 + (c_9 + c_{12})e_{12} - c_9 \lambda_6 \chi_6 - g \tag{3.39}$$

where c_7, c_8, c_9, c_{10}, c_{11}, c_{12}, λ_4, λ_5 and λ_6 are positive constants.

In order to compute total thrust, reference roll and pitch angles, Eqns. (3.37)-(3.39) are utilized to solve dynamic inversion approach. The total thrust, reference roll and pitch angles can be computed as:

$$U_1 = m\sqrt{\mu_x^2 + \mu_y^2 + (\mu_z + g)^2} \tag{3.40}$$

$$\phi_d = \left(\frac{m(\mu_x sin\psi_d - \mu_y cos\psi_d)}{U_1} \right) \tag{3.41}$$

$$\theta_d = \left(\frac{\mu_x cos\psi_d + \mu_y sin\psi_d}{\mu_z + g} \right) \tag{3.42}$$

Reference roll and pitch angles found by Eqns. (3.41)-(3.42), are inputs to the attitude control system. Furthermore, reference yaw angle can be set to any desired value.

Chapter IV

4 A New Coordination Framework for UAVs

Coordinated motion of a group of autonomous robots requires each member of the group to track reference trajectories that are dependent on the movement of the other robots in the group. Hence, coordinated motion of a group of robots will be modeled by the generation of a reference trajectory for each member in the group, that is dependent on the positions of some or all of the robots [77]. A direct result of the definition of such a task is that; the generated models of coordinated motion is scenario dependent, i.e. models for different coordinated tasks will be different. Since the generated model is scenario dependent, the scenario will be described first.

Let $Q_1, Q_2, \ldots, Q_{n-1}$ and Q_n, denote the group of n quadrotors. T represents the target object for the group. We assume that quadrotors know the position of the target, before they start their task and perceive the environment using their onboard sensors. Conditions that must be satisfied for a successful coordinated task scenario are as follows

- $Q_1, Q_2, \ldots, Q_{n-1}, Q_n$ should form a circle of radius d_{target} with T at the center.
- The quadrotors should be uniformly distributed on the final formation.

- Each Q_i should locate itself towards T once it keeps a desired distance d_{coord} from its closest neighbors and d_{target} from T.

The task scenario mentioned above can be a basis for the coordinated simple tasks. For instance, for a fire extinguishment scenario, T represents the fireplace where quadrotors can be used to extinguish the fire in coordination. Due to higher water load capacity, such a coordinated system would enable us to suppress fire more quickly. Another application of coordinated UAV control is search and rescue of injured people in earthquake territories. In this case, T can be damaged buildings and quadrotors need to decrease d_{coord} and d_{target} to achieve desired formation. Before continuing to the next stage of the task, Q_i might check if other quadrotors have succeeded the current stage of the task.

4.1 Reference Generation Model

The reference system is modeled as virtual masses that are connected with virtual springs and dampers for generating reference trajectories for each quadrotor. Every quadrotor in the group is considered as point masses denoted by $m_1,\ m_2,\ \ldots,\ m_{n-1},\ m_n$. Coordination can be specified on the basis of forces between quadrotors and the target. In this approach coordinated motion is achieved by using quadrotor-quadrotor coordination forces and target-quadrotor attraction force. The reference trajectory which is generated by virtual model is tracked by actual quadrotors with the help of attitude and position controllers. At this point, virtual reference generation can be considered as high-level controller as in Fig. 4.1 and quadrotor individual controllers (attitude and position controllers) are low-level controllers.

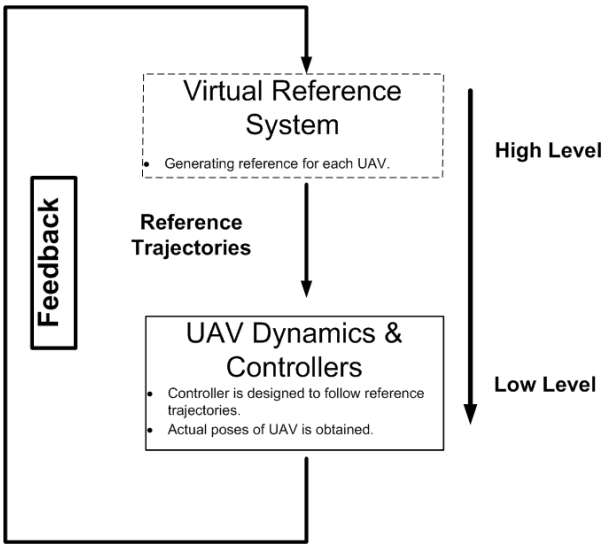

Figure 4.1: Hierarchical scheme of coordinated motion

Coordination scheme is provided by virtual bounds which are built between each m_i and its closest two neighbors. The two neighbors of m_i exert forces on m_i to keep the desired distance between each quadrotor. This distance can be considered as equilibrium length of the virtual springs and dampers which produce virtual forces between robots. We assume that m_j is the closest neighbor and m_k is the second closest neighbor of the m_i (Fig. 4.2).

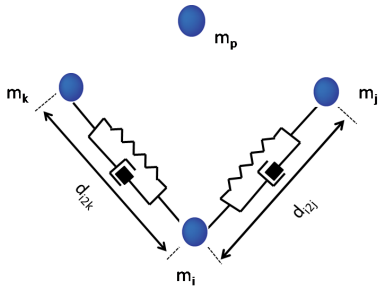

Figure 4.2: Virtual springs and dampers between a quadrotor and its two closest neighbors

In this work, we assume a planar coordination between the quadrotors where a virtual plane is defined from the orthogonal projections of the quadrotors (Fig. 4.3). The coordination force exerted on m_i from m_j and m_k is given as

$$F_{coord} = -[k_{coord}(d_{i2j} - d_{coord}) + c_{coord}((\dot{X}_i - \dot{X}_j) \bullet n_{i2j})]n_{i2j} - \ldots \\ [k_{coord}(d_{i2k} - d_{coord}) + c_{coord}((\dot{X}_i - \dot{X}_k) \bullet n_{i2k})]n_{i2k} \tag{4.1}$$

where $\bullet$ denotes vector dot product, k_{coord} and c_{coord} are the coefficients of the spring and damper. d_{i2j} is the signed distance between m_i and m_j which is projected on to the X-Y plane and d_{i2k} is the signed distance between m_i and m_k which is projected on to the X-Y plane. n_{i2j} is the unit vector from m_i to m_j, $\dot{X}_i = [\dot{x}_i \quad \dot{y}_i]^t$ is the velocity vector of virtual mass m_i. $\dot{X}_j = [\dot{x}_j \quad \dot{y}_j]^t$ is the velocity vector of virtual mass m_j, n_{i2k} is the unit vector from m_i to m_k. $\dot{X}_k = [\dot{x}_k \quad \dot{y}_k]^t$ is the velocity vector of virtual mass m_k. Moreover, d_{coord} is the coordination distance to be preserved among the masses.

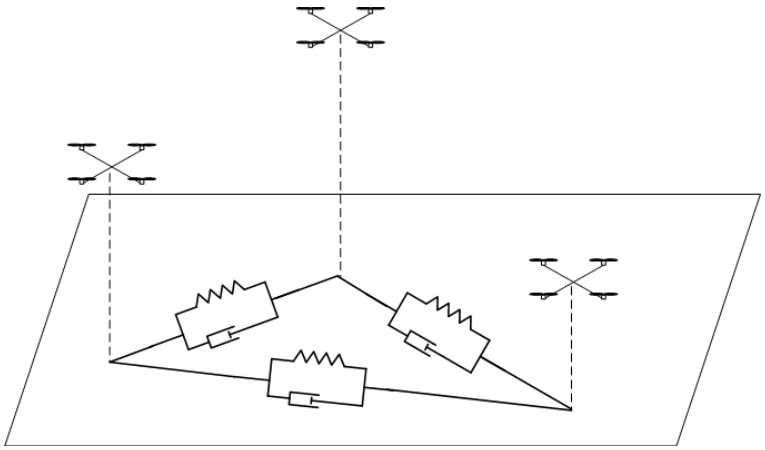

Figure 4.3: Planar distance between the quadrotors

Furthermore, target force that is exerted on each mass is modeled as the sum of spring and damper forces. The target force is defined as

$$F_{targ} = [k_{targ}(d_{i2T} - d_{targ}) + c_{targ}(\dot{X}_i \bullet n_{i2T})]n_{i2T} \tag{4.2}$$

where $\bullet$ denotes vector dot product, k_{targ} and c_{targ} are the coefficients of the spring and damper. d_{i2T} is the signed distance between m_i and target, $\dot{X}_i = [\dot{x}_i \quad \dot{y}_i]^t$ is the velocity vector of virtual mass m_i and n_{i2T} is the unit vector from m_i to target. d_{targ} is the distance to be preserved among the m_i and target.

The total force exerted on m_i is given as:

$$m_i \begin{bmatrix} \ddot{x}_i \\ \ddot{y}_i \end{bmatrix} = F_{coord} + F_{targ} \tag{4.3}$$

The reference position on X and Y axis for Q_i can be computed by double integrating the desired acceleration in Eq. (4.3). Moreover, the reference

trajectory on Z axis is generated by onboard controller of the quadrotor. In other words, reference on Z axis is given as a quintic polynomial trajectory whose initial point is the quadrotors initial point and final point is the desired height above the target. On the other hand, we may need to change the parameters which are given above to perform the coordinated tasks. In our scenario we divide coordinated motion into two stages:

i. Getting closer to T from the initial point.

ii. Forming circular distribution around T with radius d_{target}.

In the first stage, coordinated motion of quadrotors is the most important issue. Until the end of the first stage, F_{coord} is dominant for moving robots together. However, target force, F_{target}, is also important to move the robots toward T. When any robot in the group, Q_i, is close to T at a certain distance, d_{break}, the importance of target force increases. In other words, k_{coord} is decreased to k_{near}, which is smaller than k_{targ} for achieving the final formation. Moreover, coordination distance, d_{coord} must be changed to d_{near} for generating uniform circular formation (Fig 4.4).

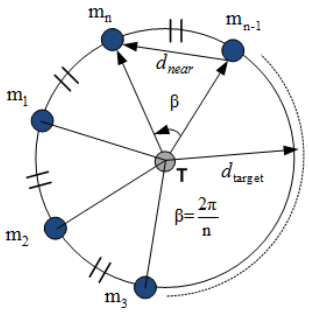

Figure 4.4: Uniform distribution of masses on the formation circle around T

d_{near} can be calculated from the final distribution as follows [78]:

$$d_{near} = d_{target}\sqrt{2(1 - cos(2\pi/n))}. \tag{4.4}$$

Spring coefficient, k_{coord}, is changed as a continuous function of d_i2T as in [78]:

$$k_{coord} = k_{near} + \frac{k_{far} - k_{near}}{1 + exp(\alpha(d_{break} - d_i2T + \gamma))} \tag{4.5}$$

where $\alpha > 0$ and $\gamma > 0$ are constants, $0 \leq k_{coord} \leq 1$, d_{i2T} is the signed distance between m_i and the target, k_{far} and k_{near} are spring coefficients that are used in stage 1 and 2.

Chapter V

5 Simulation Results and Discussion

In order to verify proposed formation control method, several simulations are carried out in Matlab/Simulink environment. In simulations, three and five quadrotors are considered for a coordinated task defined by a circular formation around the target.

5.1 Coordinated Motion of Three Quadrotors

This simulation was run for a group of three quadrotor. In the this scenario, the quadrotors are placed at different corners of a room on the ground where $Q_1 = [5 \quad 0 \quad 0]^T$, $Q_2 = [5 \quad -5 \quad 0]^T$ and $Q_3 = [-5 \quad -5 \quad 0]^T$ while T is placed at the center of the room, $T = [0 \quad 0 \quad 0]^T$. In this simulation, quadrotors are not subject to any external disturbances. Moreover, the coordinated motion parameters in the simulations are set in Table 5.1. The trajectories of quadrotors which are generated by proposed virtual reference model are shown in Figs. (5.1 - 5.4). In Fig. 5.1 and 5.2, quadrotors are controlled by using classical PID controller whereas in Fig. 5.3 and 5.4 quadrotors are controlled by using integral backstepping (IB) controllers. It can be observed that they approach each other and move towards T in a coordinated manner. As the distance between each Q_i and T falls below d_{break}, virtual bonds among the quadrotors are relaxed and F_{targ} becomes dominant. When they

Table 5.1: Coordinated Motion Model Parameters for Simulations

Parameter Name	Value
c_{coord}	5.0
d_{coord}	1.0
k_{targ}	10.0
c_{targ}	3.5
d_{targ}	2.0
k_{far}	10.0
k_{near}	2.0
α	10.0
γ	0.5
d_{break}	$1.5d_{targ}$

are close to T, they keep mutual distances of d_{near}, then they spread around the circle. Finally, the group reach desired formation at 5 meters above the target indicated as star in figures.

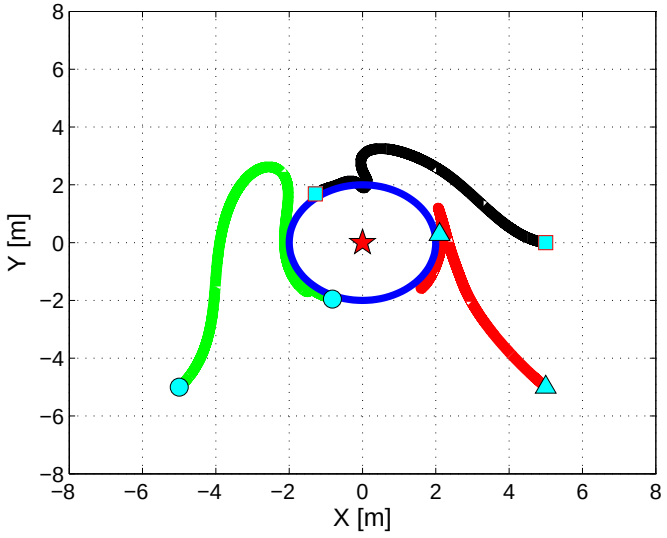

Figure 5.1: PID Controlled UAVs Trajectories on X-Y Plane

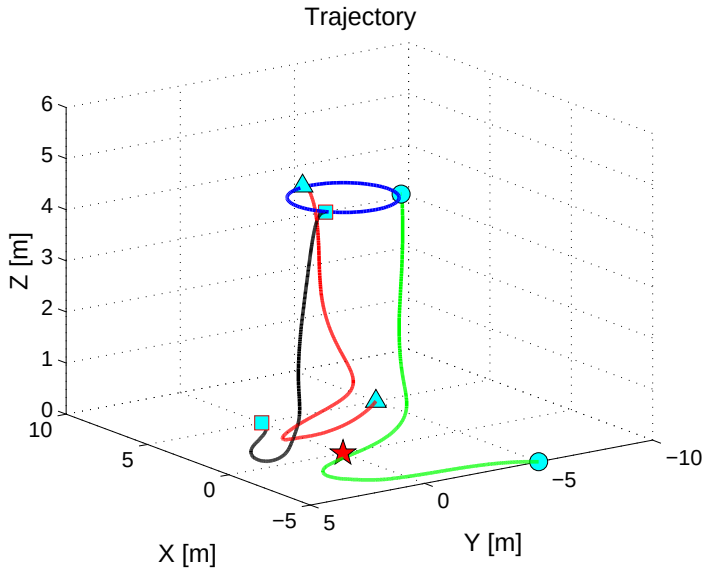

Figure 5.2: PID Controlled UAVs Trajectories in 3D

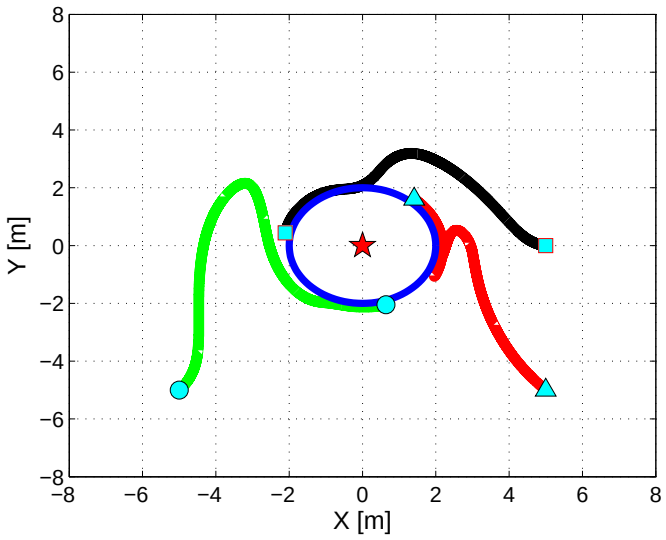

Figure 5.3: IB Controlled UAVs Trajectories on X-Y Plane

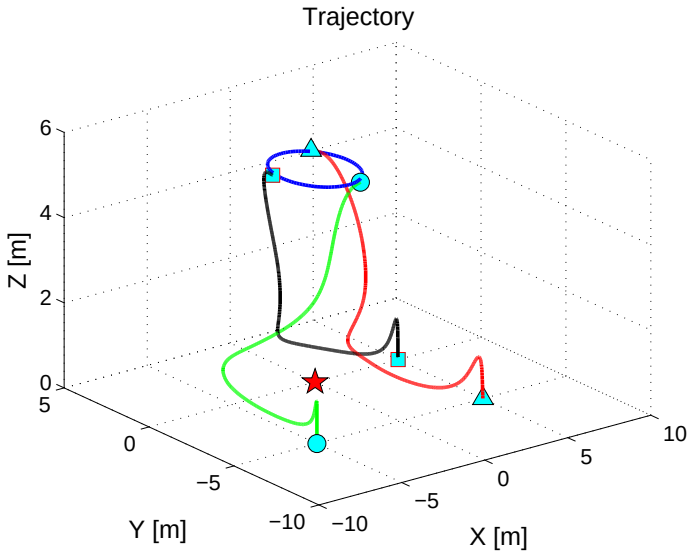

Figure 5.4: IB Controlled UAVs Trajectories in 3D

Furthermore, attitude angles and positions of quadrotors are shown in Figs. 5.5, 5.6 and 5.7. As can be seen from the figures, quadrotors are able to track reference trajectories successfully. Although quadrotors are not subject to external disturbance, integral backstepping controllers perform better than PID controllers.

RMS values of attitude and position tracking errors are tabulated in Table 5.2. Integral backstepping controllers are able to keep the attitude and position tracking errors under 0.0035 rad and 0.013 m, whereas the tracking errors increase up to 0.012 rad and 0.019 m in PID controllers. However, quadrotors which have integral backstepping controllers have larger errors along the Z axis. The reason is that quadrotors first vertically take-off and then track the reference trajectory. This causes bigger RMS error values along the Z axis when it is compared with errors along X and Y axes.

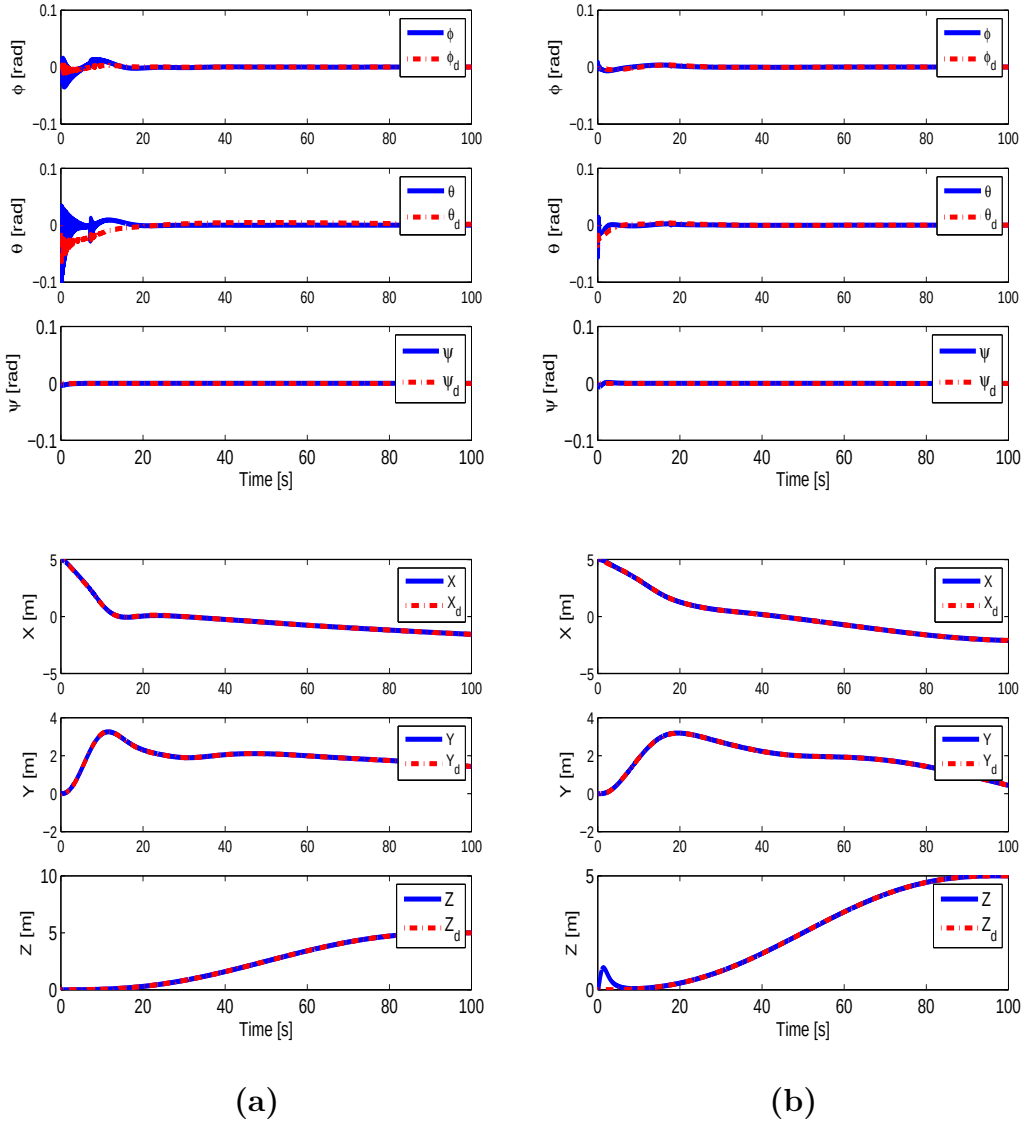

Figure 5.5: Attitude and Position tracking of the first quadrotor (Q_1) using (a) PID Control, (b) IB Control under no external disturbance.

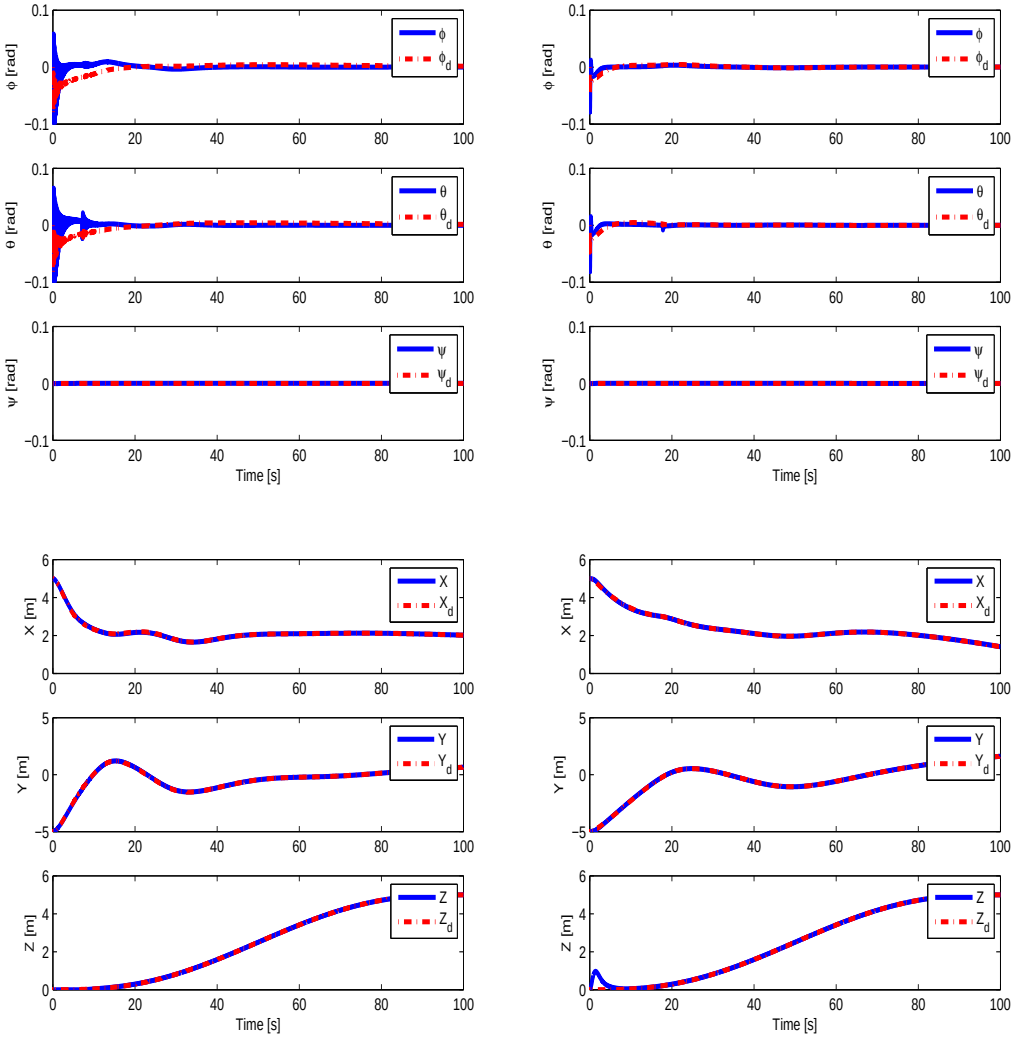

Figure 5.6: Attitude and Position tracking of the second quadrotor (Q_2) using (a) PID Control, (b) IB Control under no external disturbance.

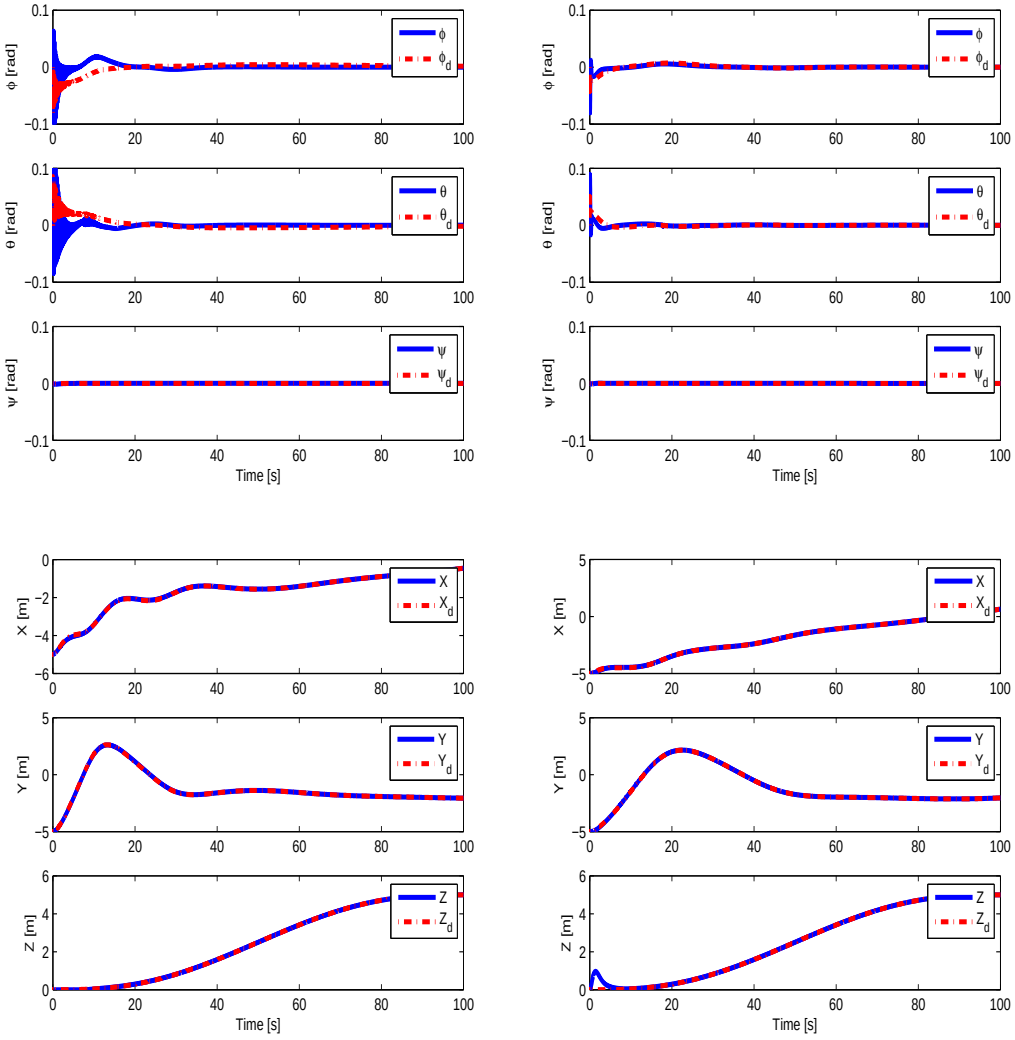

Figure 5.7: Attitude and Position tracking of the third quadrotor (Q_3) using (a) PID Control, (b) IB Control under no external disturbance.

In the second scenario, quadrotors are located at the same places as in the first scenario, and T is placed at the center of the room. In this scenario quadrotors are subject to external disturbances. These external disturbances are generated as forces and moments produced by wind that is modeled using

Table 5.2: RMS Errors for PID and IB under no External Disturbance

Error	1. IB	1. PID	2. IB	2. PID	3. IB	3. PID
e_ϕ (rad)	0.0007	0.0031	0.0026	0.0097	0.0025	0.0104
e_θ (rad)	0.0025	0.0099	0.0029	0.0100	0.0032	0.0114
e_ψ (rad)	0.0005	0.0003	0.0003	0.0004	0.0009	0.0002
e_X (m)	0.0117	0.0173	0.0128	0.0167	0.0128	0.0166
e_Y (m)	0.0032	0.0067	0.0118	0.0168	0.0115	0.0187
e_Z (m)	0.1311	0.0004	0.1310	0.0034	0.1310	0.0040

Dryden Wind-Gust model [79] and they are depicted in Fig. 5.8.

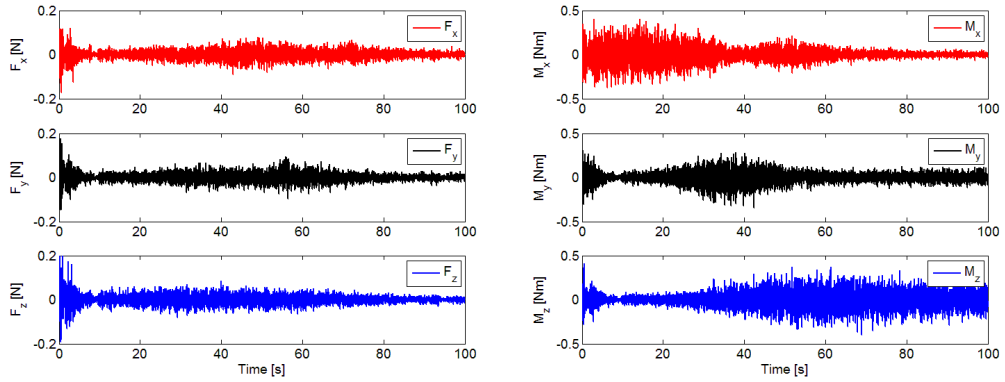

(a) (b)

Figure 5.8: External disturbance forces and moments

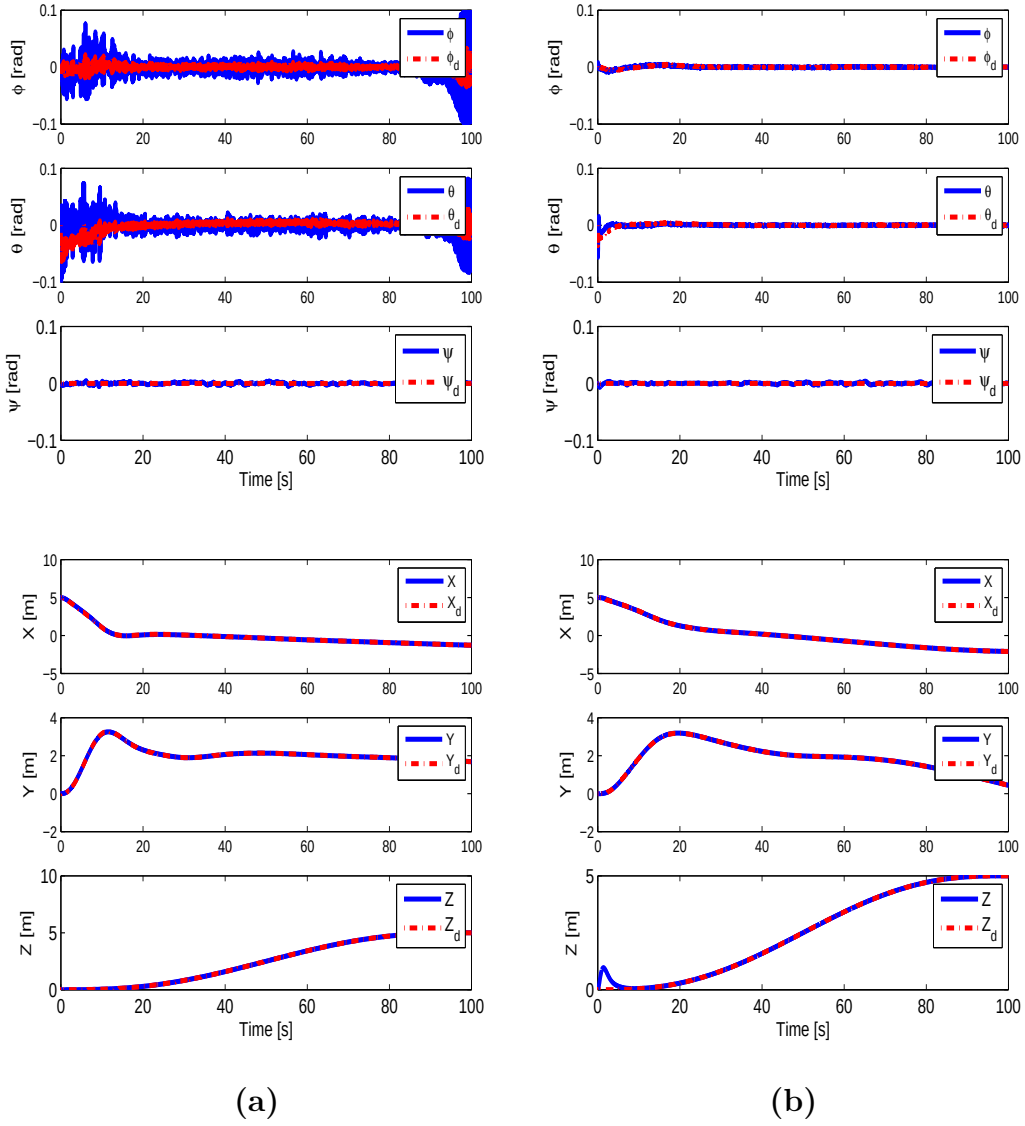

Figure 5.9: Attitude and Position tracking of the first quadrotor (Q_1) using (a) PID Control, (b) IB Control under external disturbance.

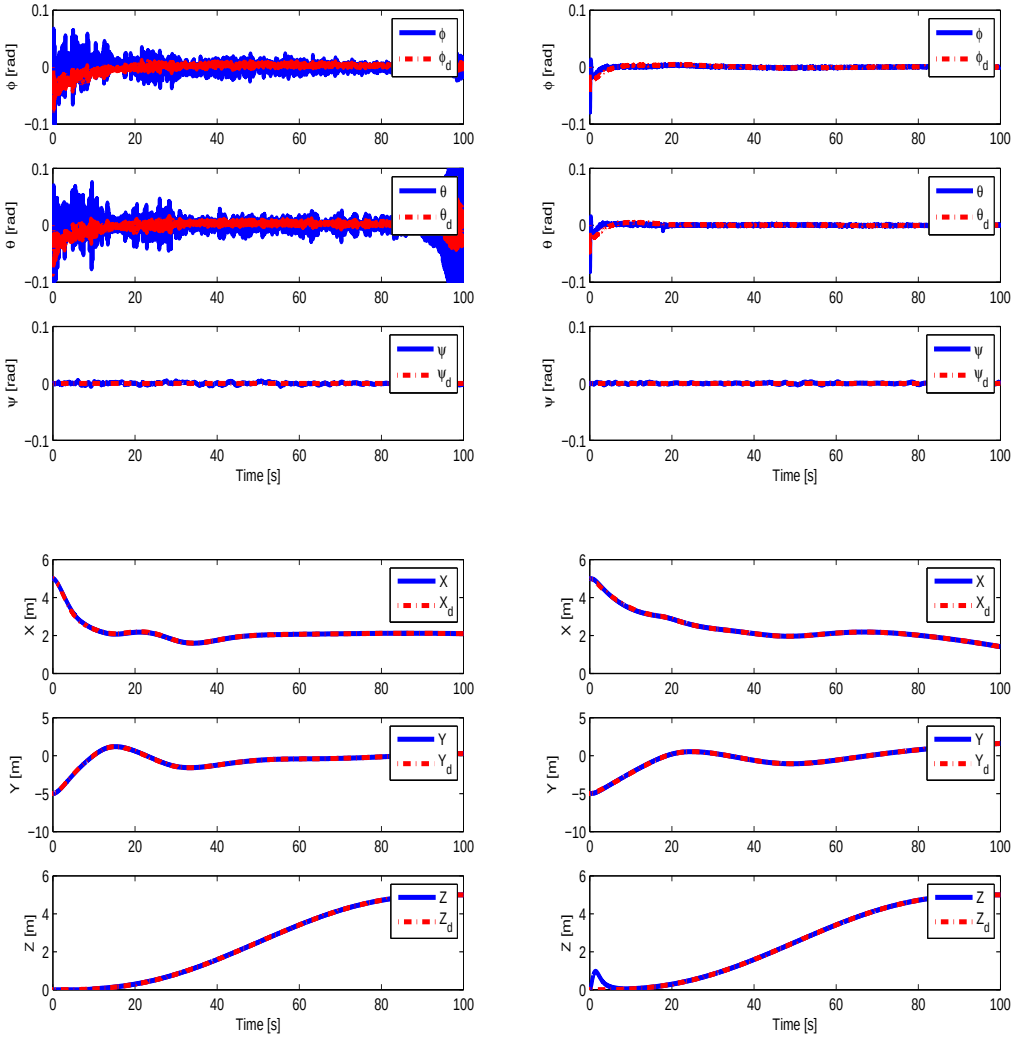

Figure 5.10: Attitude and Position tracking of the second quadrotor (Q_2) using (a) PID Control, (b) IB Control under external disturbance.

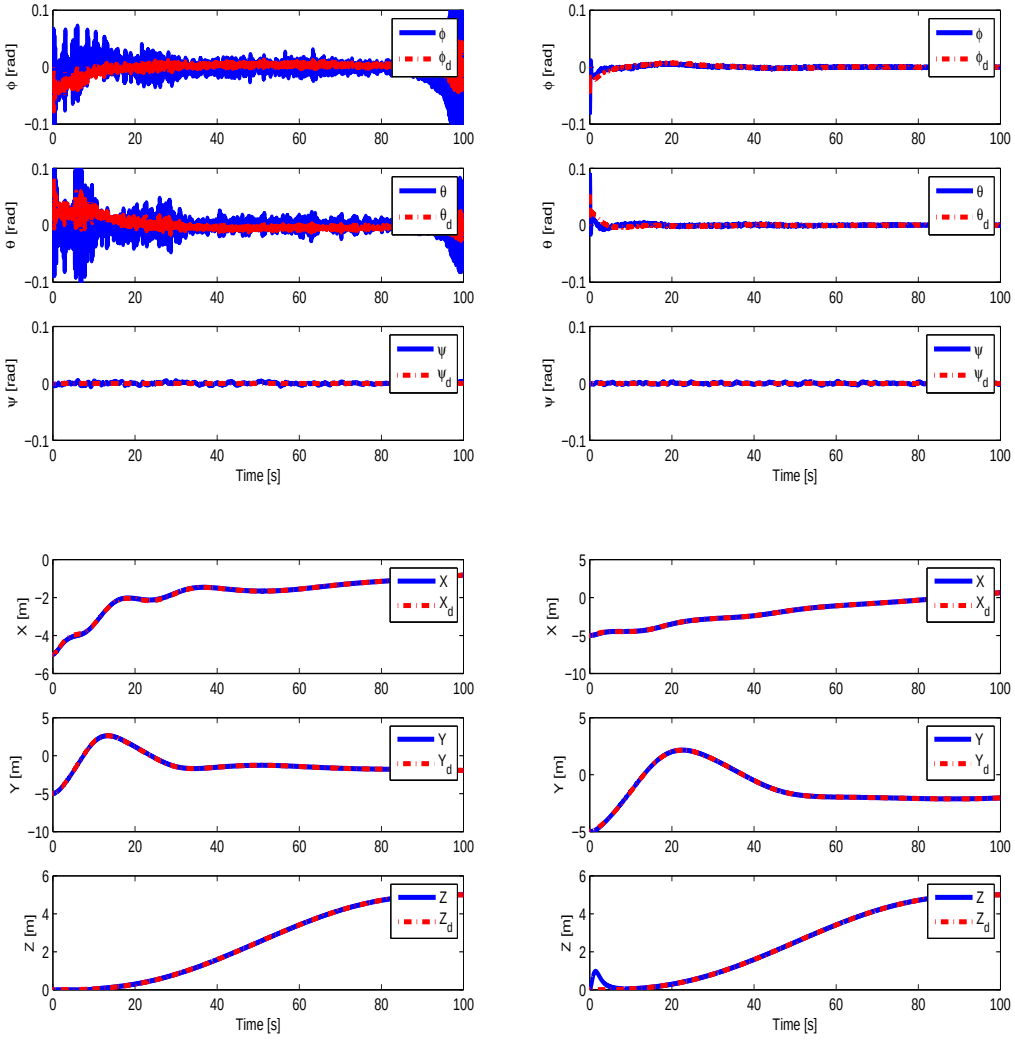

Figure 5.11: Attitude and Position tracking of the third quadrotor (Q_3) using (a) PID Control, (b) IB Control under external disturbance.

Furthermore, attitude angles and positions of quadrotors are shown in Figs. 5.9, 5.10 and 5.11. In light of these graphs, quadrotors are able to track reference trajectories successfully despite the external disturbance. Moreover, integral backstepping controllers lead to smaller attitude and position

Table 5.3: RMS Errors for PID and IB under External Disturbance Generated by Dryden Wind Model

Error	1. IB	1. PID	2. IB	2. PID	3. IB	3. PID
e_ϕ (rad)	0.0009	0.0166	0.0027	0.0131	0.0026	0.0217
e_θ (rad)	0.0026	0.0161	0.0030	0.0225	0.0032	0.0199
e_ψ (rad)	0.0013	0.0016	0.0010	0.0016	0.0012	0.0017
e_X (m)	0.0117	0.0156	0.0128	0.0144	0.0127	0.0179
e_Y (m)	0.0033	0.0065	0.0118	0.0161	0.0115	0.0183
e_Z (m)	0.1311	0.0020	0.1310	0.0039	0.1310	0.0049

tracking errors. More precisely both controllers can keep the attitude and position tracking errors in the vicinity of 0.02 rad and 0.02 m respectively.

RMS values of integral backstepping and PID attitude and position controllers tracking errors are tabulated in Table 5.3. Moreover, integral backstepping and PID position tracking errors are close but there are huge differences in attitude angle RMS error values. Table 5.3 demonstrates the performance of integral backstepping and PID controllers against external disturbance. Notice that although both controller approaches are able to keep attitude tracking errors below 0.02 rad and position tracking errors in the vicinity of 0.02 m, integral backstepping approach has worse performance along Z axis than PID based approach as before.

To conclude, the two simulation scenarios demonstrate that both control approaches lead to comparably successful results when there is no external disturbance. However, integral backstepping controllers perform better than PID based controllers if the aerial vehicle is subject to external disturbance.

5.2 Coordinated Motion of Five Quadrotors

This simulation was run for a group of five quadrotors. The quadrotors are placed at different corners of a room on the ground where $Q_1 = [5 \quad 0 \quad 0]^T$, $Q_2 = [5 \quad 5 \quad 0]^T$, $Q_3 = [0 \quad 5 \quad 0]^T$, $Q_4 = [-5 \quad 0 \quad 0]^T$ and $Q_5 = [0 \quad -5 \quad 0]^T$ while T is placed at center of the room, $T = [0 \quad 0 \quad 0]^T$ and they are not subject to any external disturbances. The trajectories of quadrotors which are generated by virtual reference model are shown in Figs. (5.12 - 5.15). In Fig. 5.12 and 5.13, quadrotors are controlled by using classical PID controller while in Fig. 5.14 and 5.15 quadrotors are controlled by using integral backstepping (IB) controllers. It can be observed that they approach each other and move in a coordinated fashion towards T. As the distance between each Q_i and T falls below d_{break}, they keep mutual distances of d_{near}. Finally, they take the form of a pentagon with sides equal to d_{near} at 5 m height.

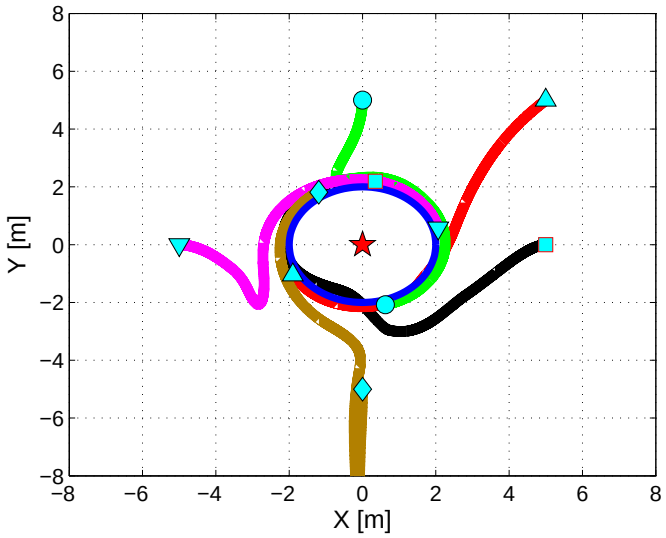

Figure 5.12: PID Controlled UAVs Trajectories on X-Y Plane

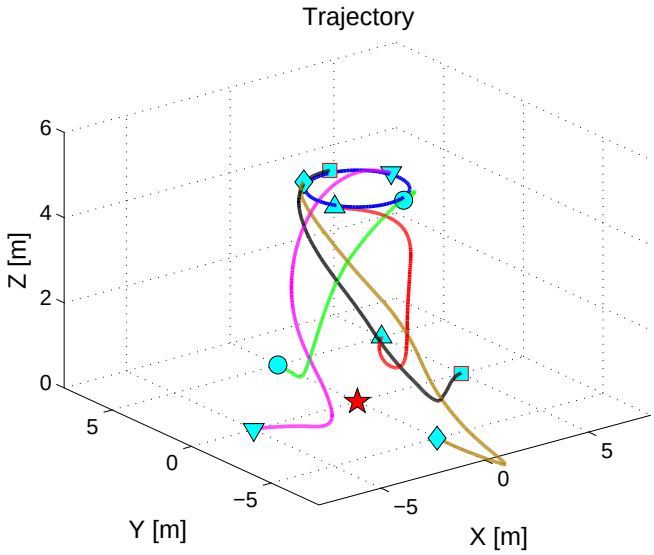

Figure 5.13: PID Controlled UAVs Trajectories in 3D

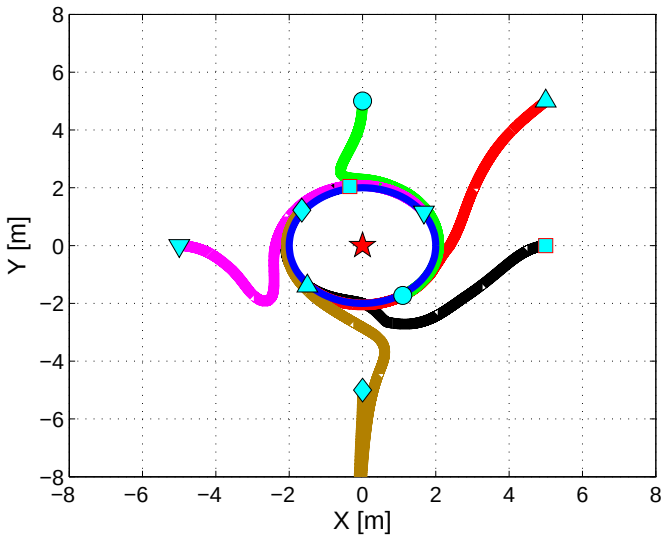

Figure 5.14: IB Controlled UAVs Trajectories on X-Y Plane

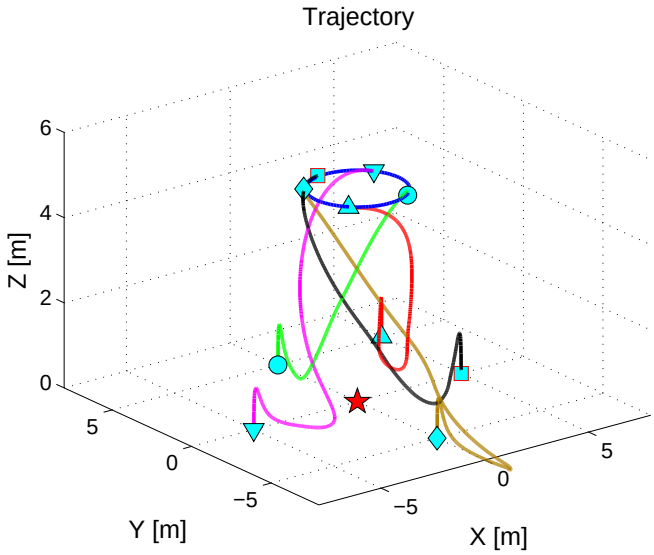

Figure 5.15: IB Controlled UAVs Trajectories in 3D

Moreover, attitude angles and positions of quadrotors are shown in Figs. 5.16 - 5.20. In light of these graphs, quadrotors are able to track reference trajectories successfully. Although quadrotors are not subject to external disturbances integral backstepping controllers have slightly better performance than the PID controllers.

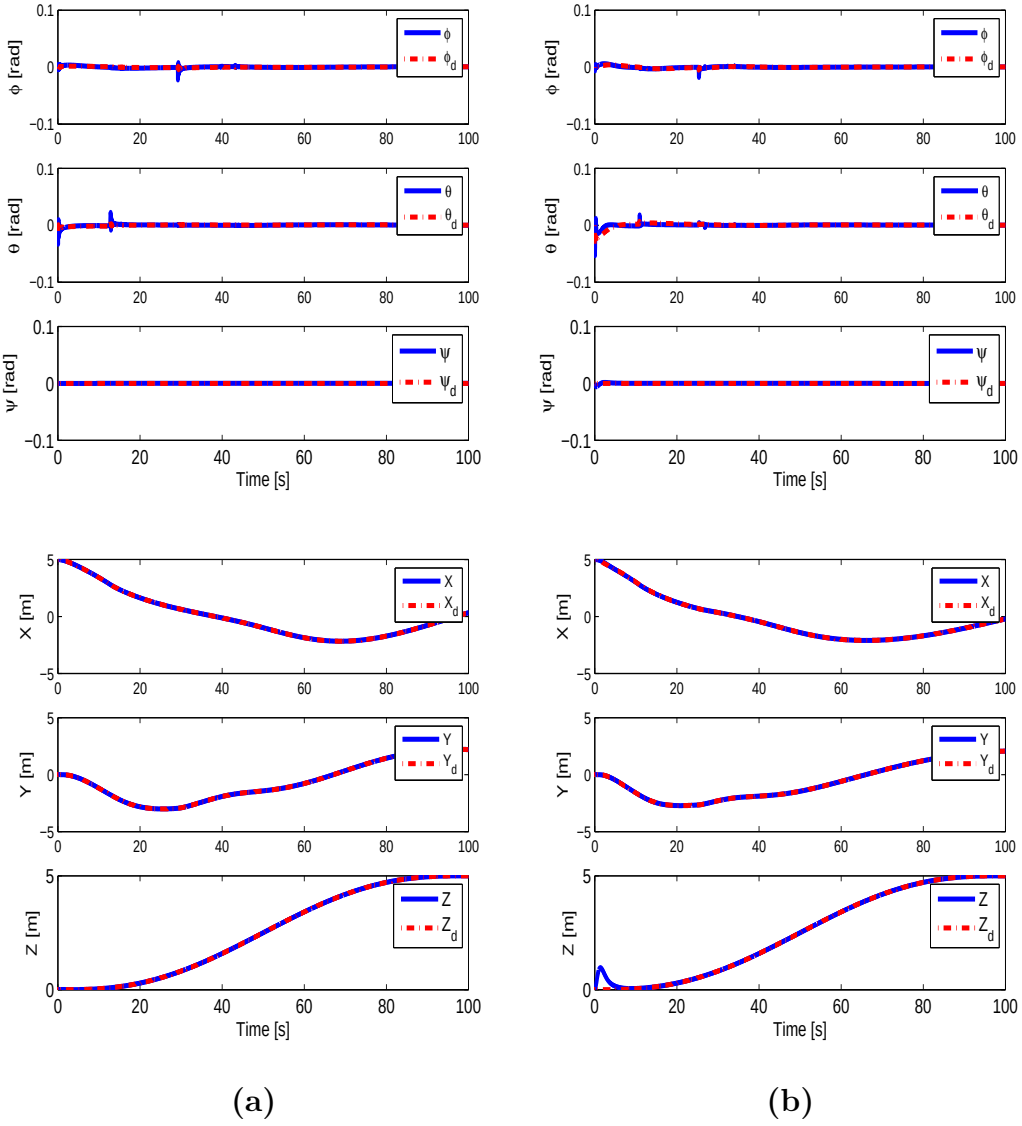

Figure 5.16: Attitude and Position tracking of the first quadrotor (Q_1) using (a) PID Control, (b) IB Control under no external disturbance.

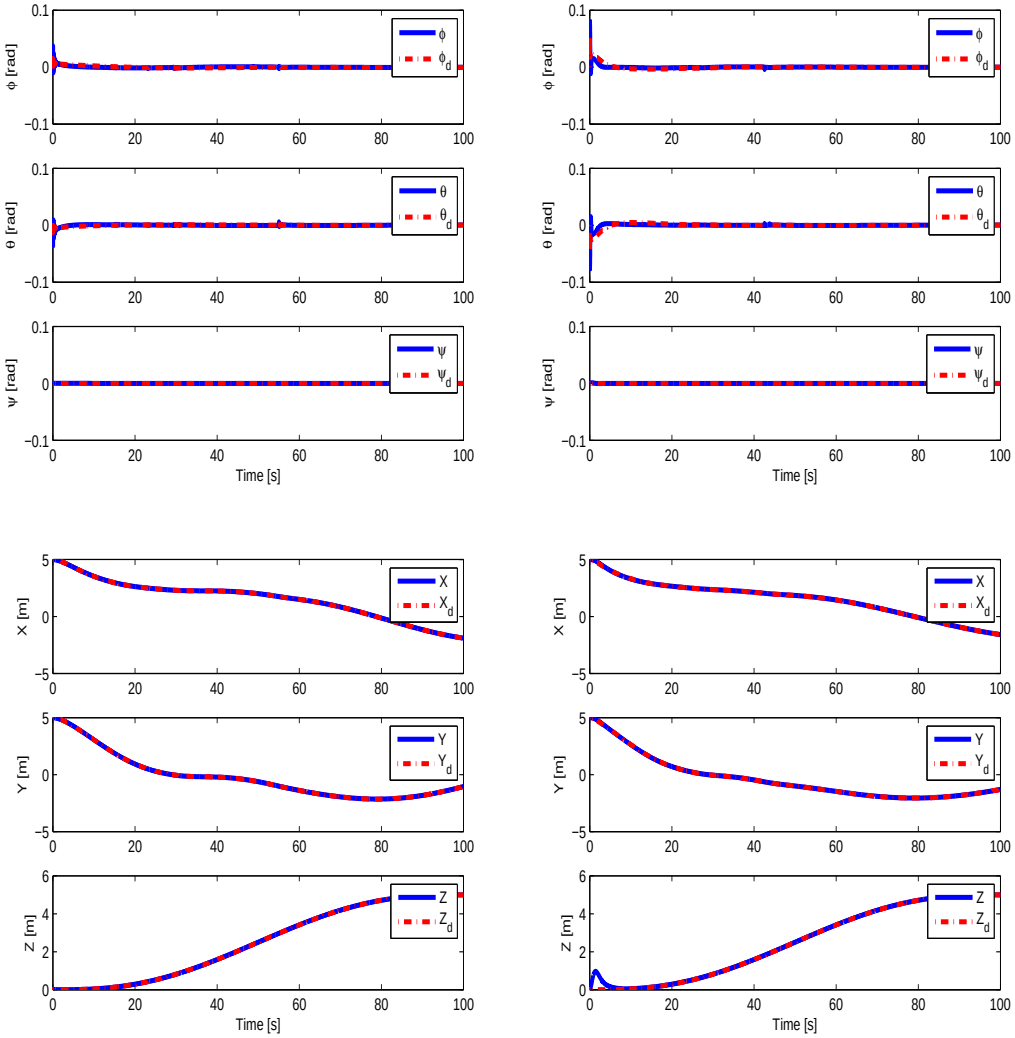

Figure 5.17: Attitude and Position tracking of the second quadrotor (Q_2) using (a) PID Control, (b) IB Control under no external disturbance.

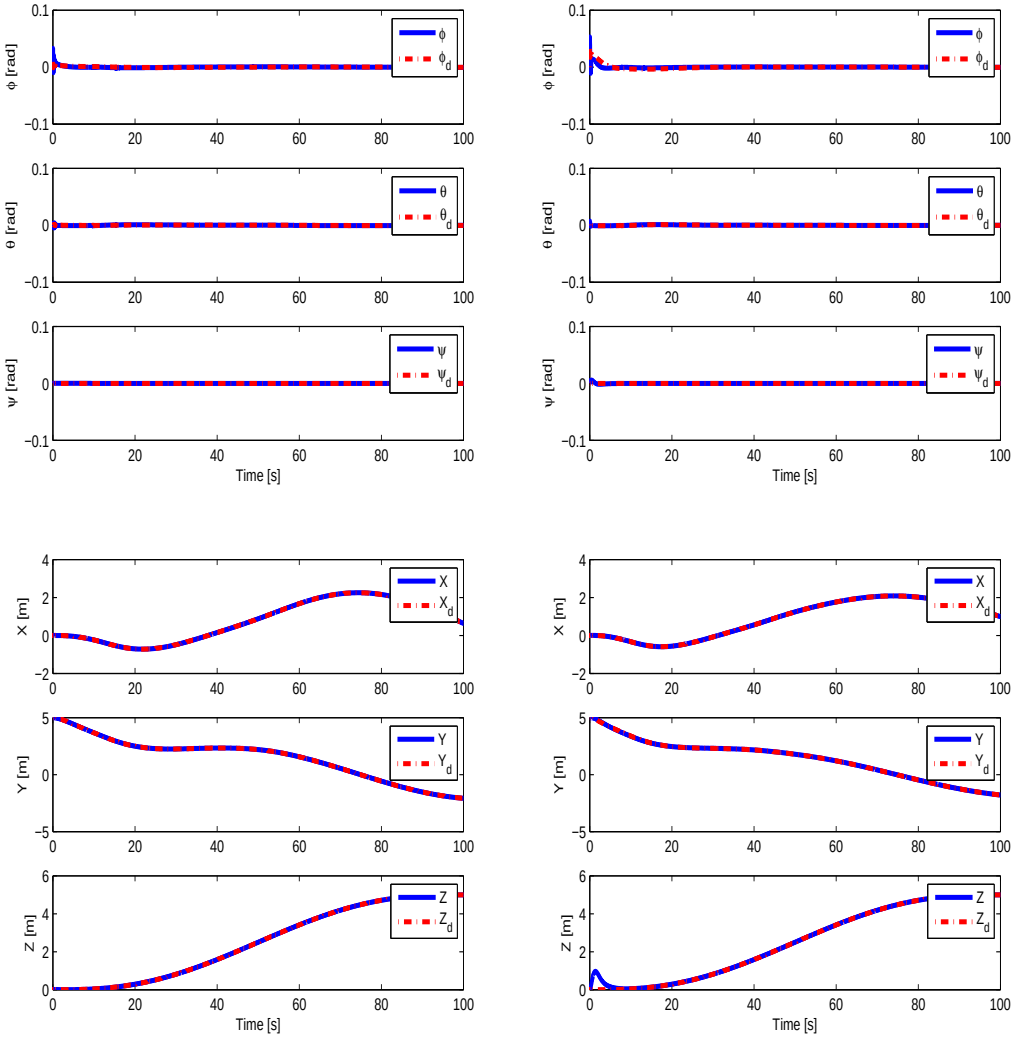

Figure 5.18: Attitude and Position tracking of the third quadrotor (Q_3) using (a) PID Control, (b) IB Control under no external disturbance.

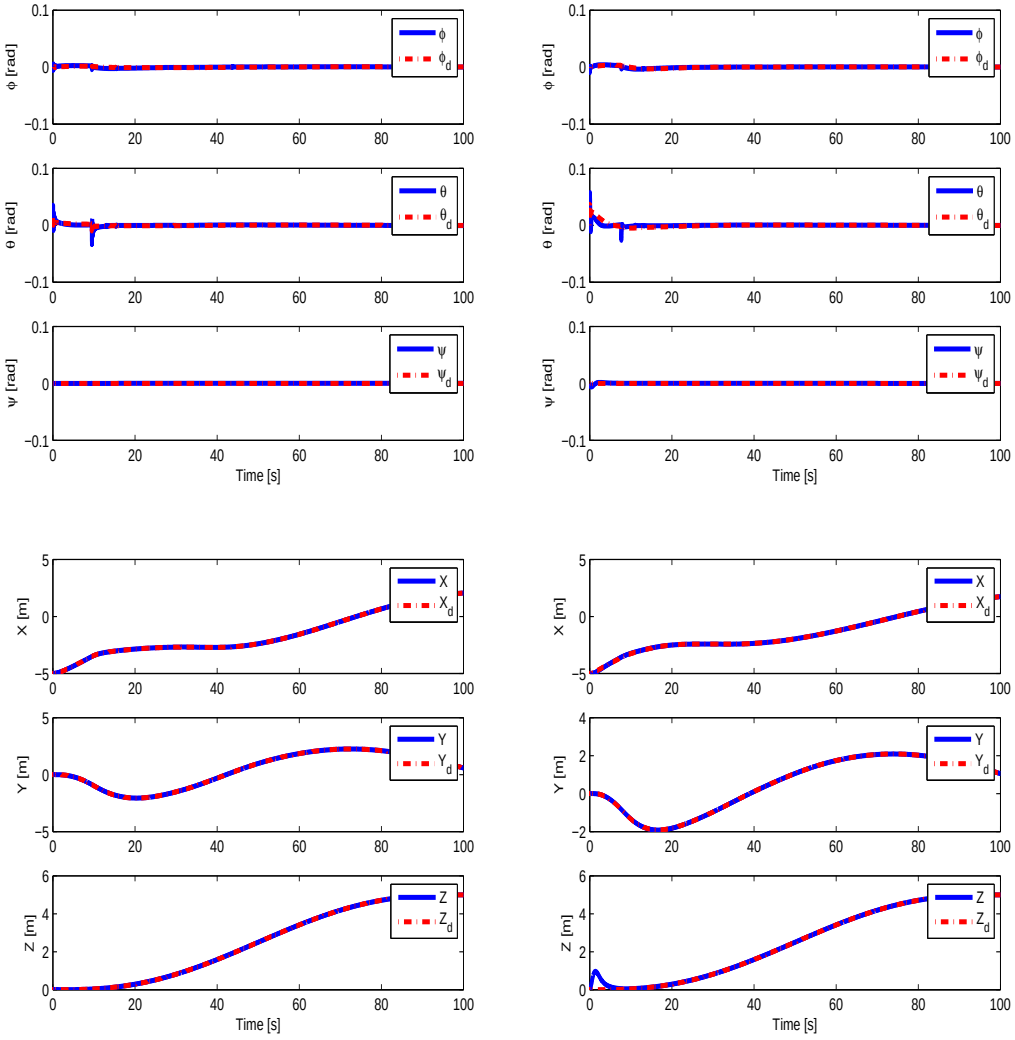

Figure 5.19: Attitude and Position tracking of the forth quadrotor (Q_4) using (a) PID Control, (b) IB Control under no external disturbance.

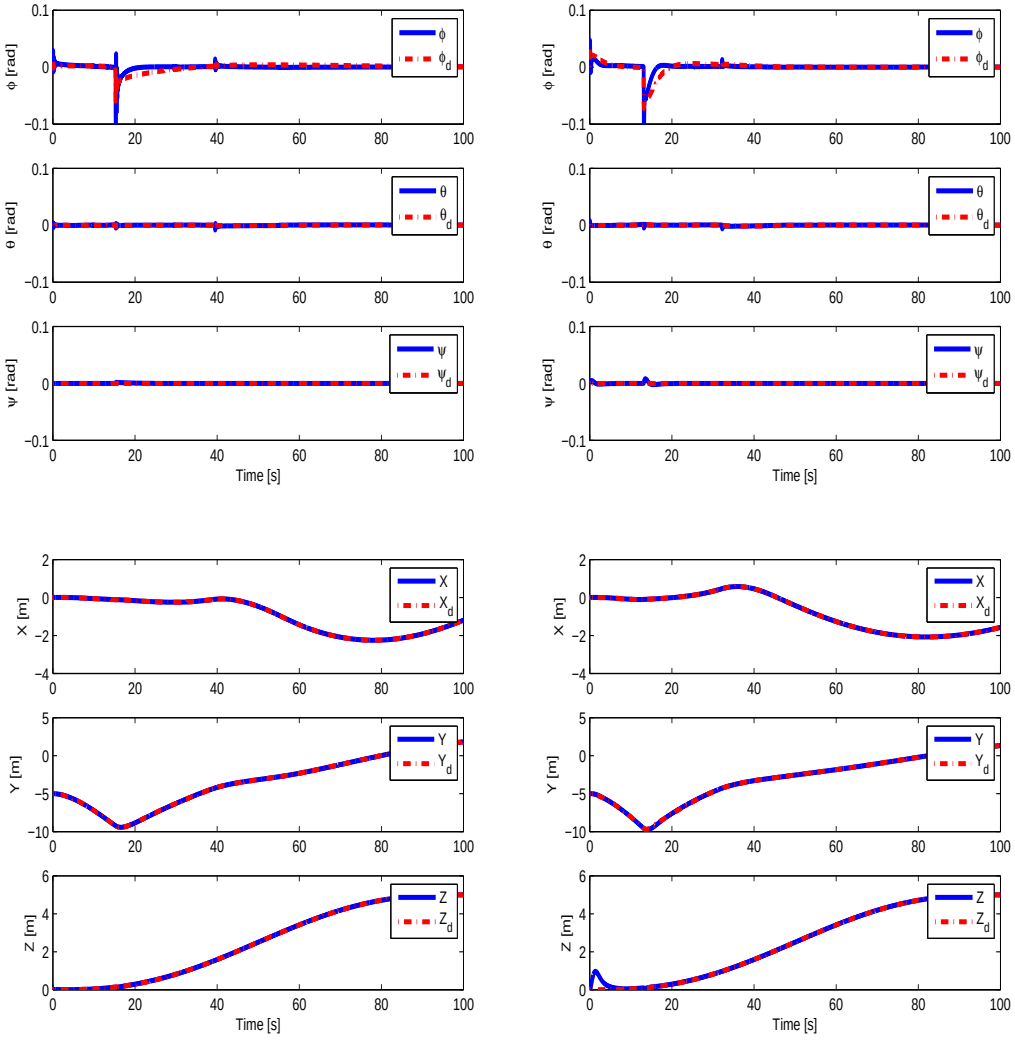

Figure 5.20: Attitude and Position tracking of the fifth quadrotor (Q_5) using (a) PID Control, (b) IB Control under no external disturbance.

RMS values of attitude and position tracking errors are tabulated in Table 5.4 and Table 5.5. According to Table 5.4, integral backstepping keeps attitude tracking errors below 0.0015 rad and position tracking errors in the vicinity of 0.003 m, error along the Z axis is larger as before. In light of

Table 5.5, PID based method keeps attitude tracking errors below 0.003 rad and position tracking errors in the vicinity of 0.013 m. The results under no external disturbance are close, but integral backstepping controllers lead to slightly less error compared to PID controllers.

Table 5.4: RMS Errors for IB under no External Disturbance

Error	1. IB	2. IB	3. IB	4. IB	5. IB
e_ϕ (rad)	0.0009	0.0013	0.0010	0.0008	0.0050
e_θ (rad)	0.0012	0.0012	0.0003	0.0013	0.0004
e_ψ (rad)	0.0001	0.0001	0.0001	0.0001	0.0001
e_X (m)	0.0015	0.0019	0.0007	0.0019	0.0007
e_Y (m)	0.0019	0.0021	0.0014	0.0019	0.0028
e_Z (m)	0.1311	0.1310	0.1311	0.1310	0.1311

Table 5.5: RMS Errors for PID under no External Disturbance

Error	1. PID	2. PID	3. PID	4. PID	5. PID
e_ϕ (rad)	0.0009	0.0026	0.0024	0.0006	0.0055
e_θ (rad)	0.0025	0.0029	0.0002	0.0027	0.0004
e_ψ (rad)	0.0005	0.0001	0.0005	0.0005	0.0008
e_X (m)	0.0117	0.0131	0.0007	0.0123	0.0012
e_Y (m)	0.0031	0.0115	0.0115	0.0027	0.0029
e_Z (m)	0.0022	0.0011	0.0014	0.0013	0.0028

In the second scenario, quadrotors are located at the same places in the first scenario and also T is placed at the center of the room. In this simulation quadrotors are subject to external disturbances. Furthermore, attitude angles and positions of quadrotors are shown in Figs. 5.21 - 5.25. It is clear from these figures that quadrotors follow the desired references quite successfully despite the external disturbances. Integral backstepping controllers perform better than PID controllers. Moreover, integral backstepping method is more responsive to reference trajectory variation. Hence, it leads to less error compared to PID controller.

RMS values of attitude and position tracking errors are tabulated in Table 5.6 and Table 5.7. According to Table 5.6, integral backstepping keeps attitude tracking errors below 0.006 rad and position tracking errors in the vicinity of 0.0045 m, error along the Z axis is larger as before. In Table 5.7, PID based method keeps attitude tracking errors below 0.01 rad and position tracking errors in the vicinity of 0.03 m. These results demonstrate that integral backstepping controllers perform better than PID controllers if the aerial vehicle is subject to external disturbance.

To sum up, the two simulation scenarios demonstrate that both control approaches lead to comparably successful results when there is no external disturbance. However, integral backstepping controllers have better performance than PID controllers, if the aerial vehicle is subject to external disturbance.

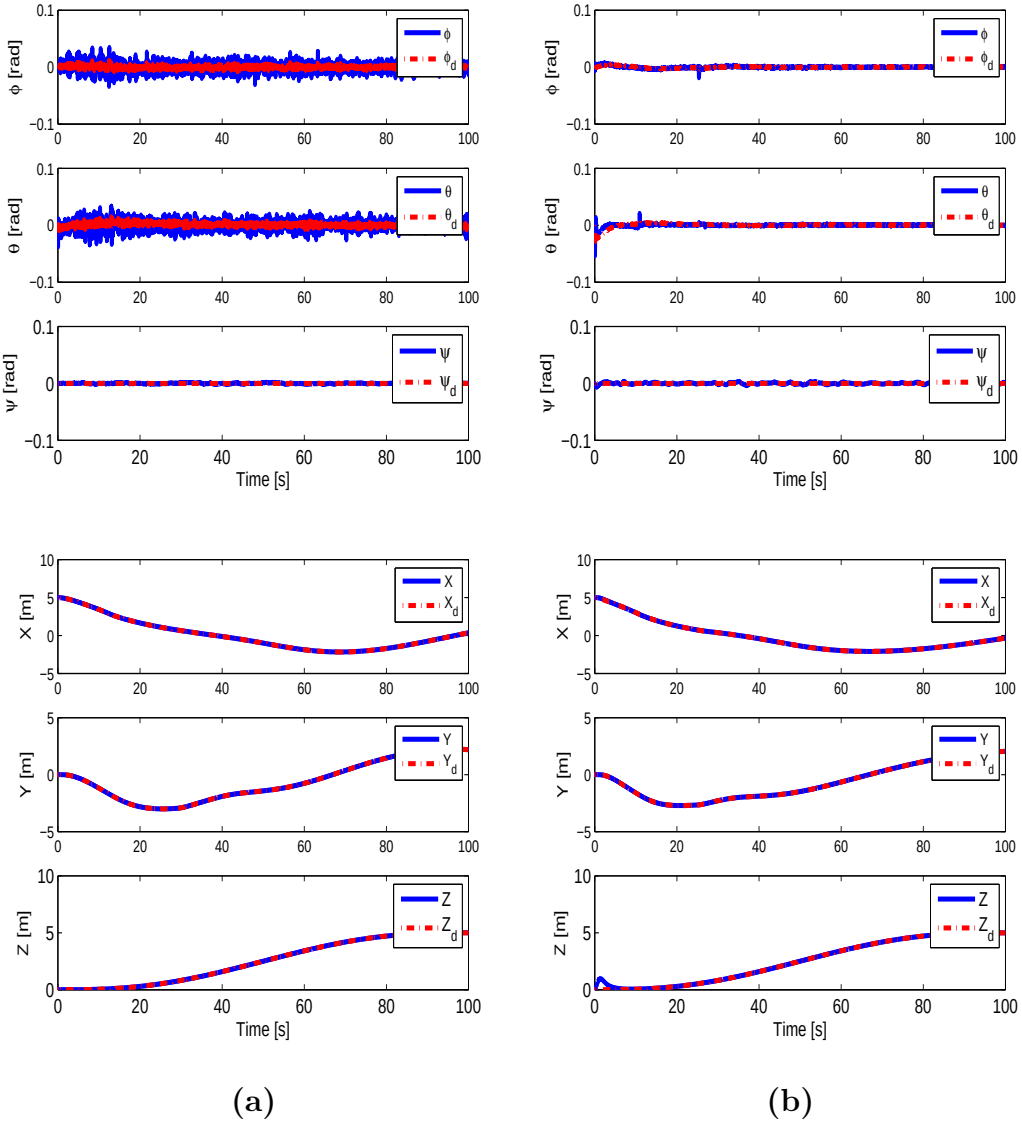

Figure 5.21: Attitude and Position tracking of the first quadrotor (Q_1) using (a) PID Control, (b) IB Control under external disturbance.

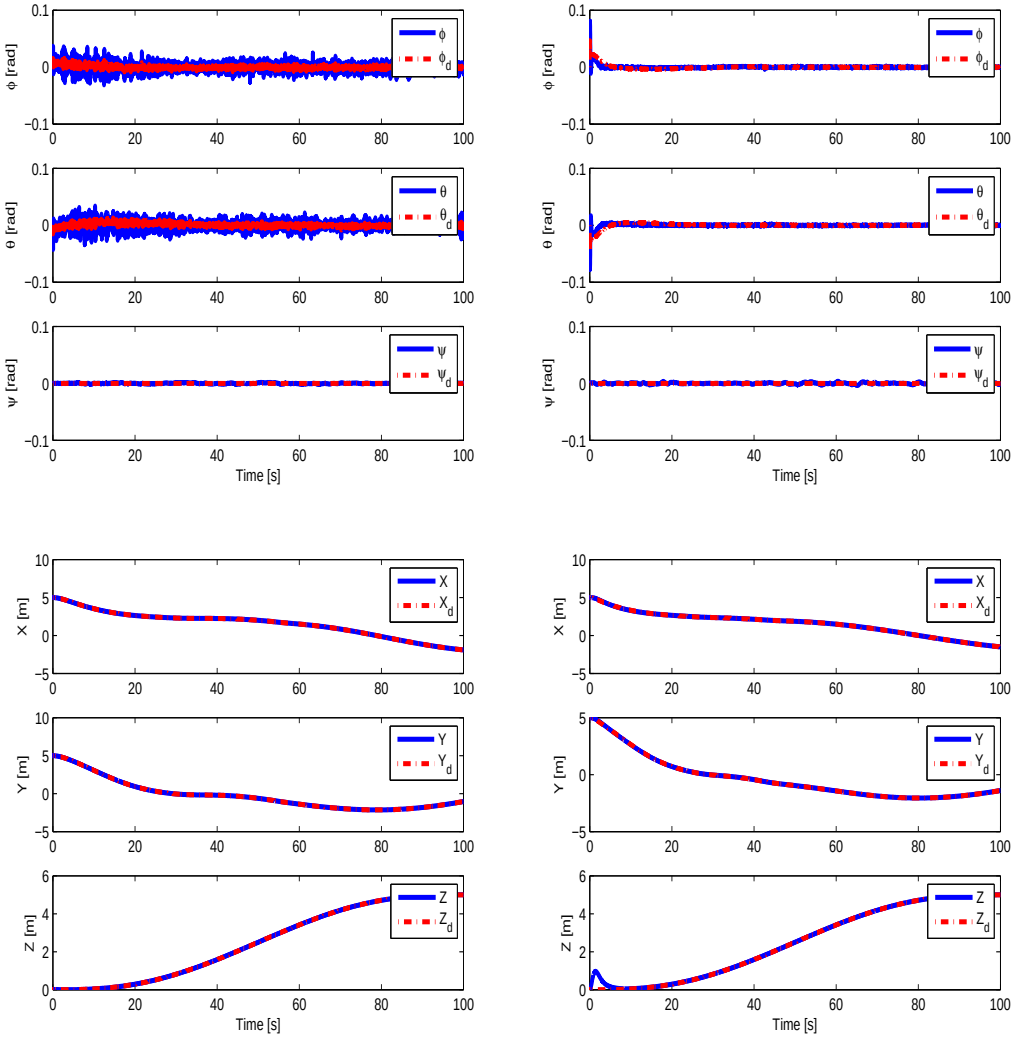

Figure 5.22: Attitude and Position tracking of the second quadrotor (Q_2) using (a) PID Control, (b) IB Control under external disturbance.

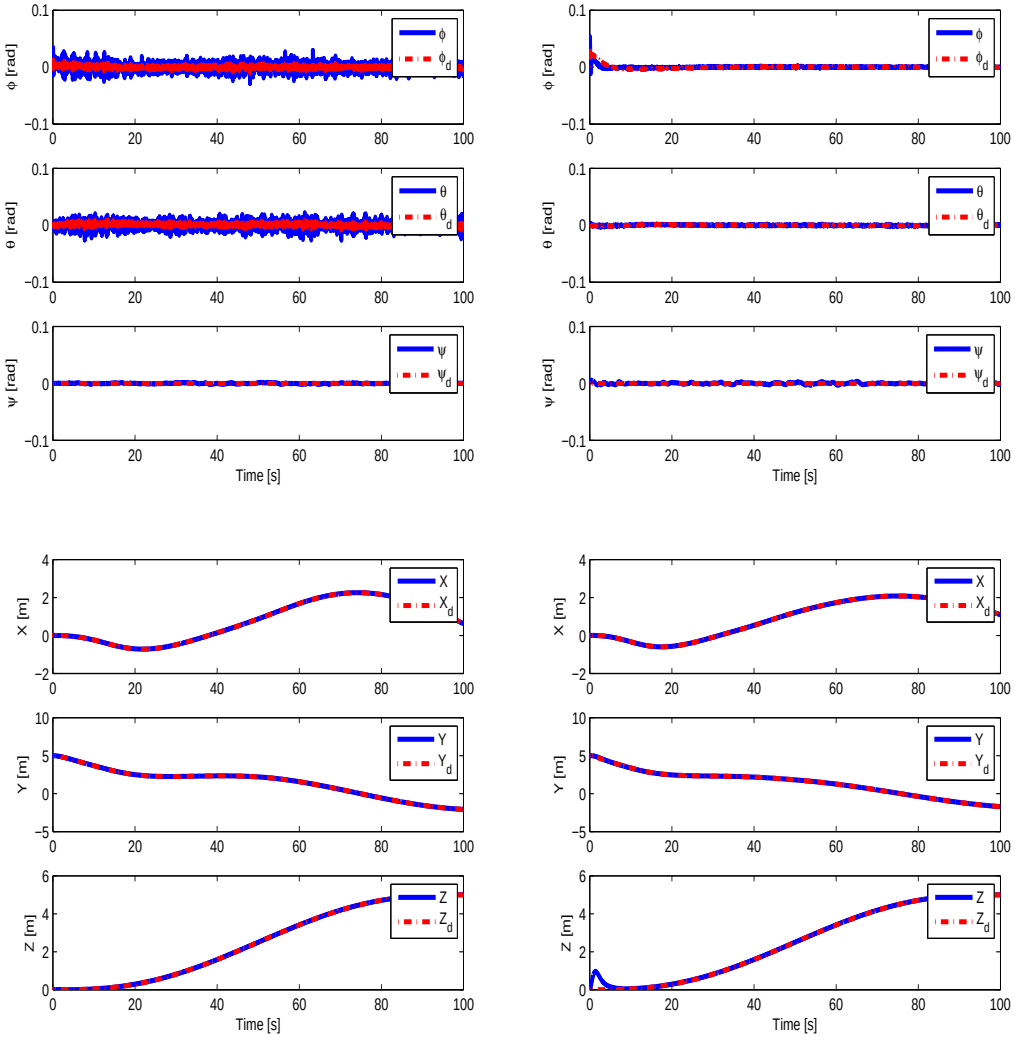

Figure 5.23: Attitude and Position tracking of the third quadrotor (Q_3) using (a) PID Control, (b) IB Control under external disturbance.

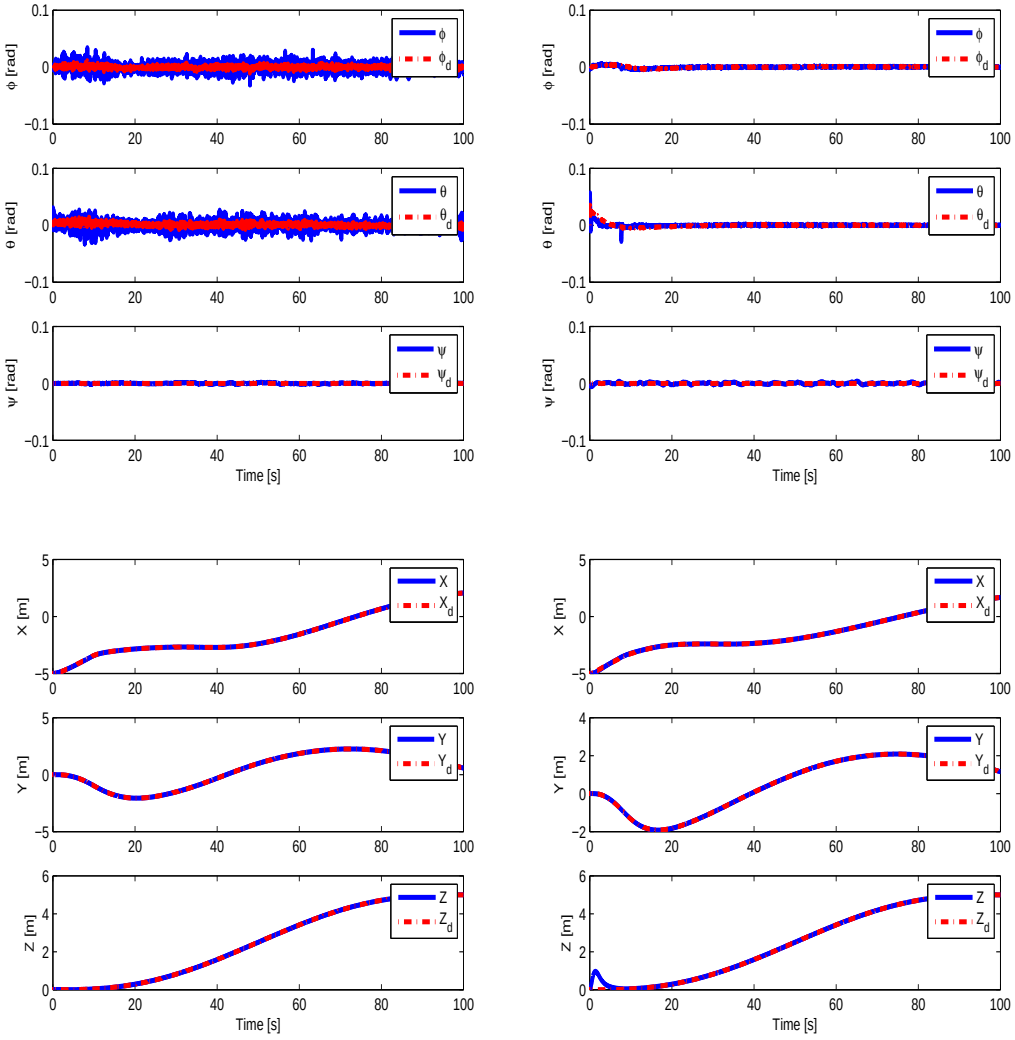

Figure 5.24: Attitude and Position tracking of the forth quadrotor (Q_4) using (a) PID Control, (b) IB Control under external disturbance.

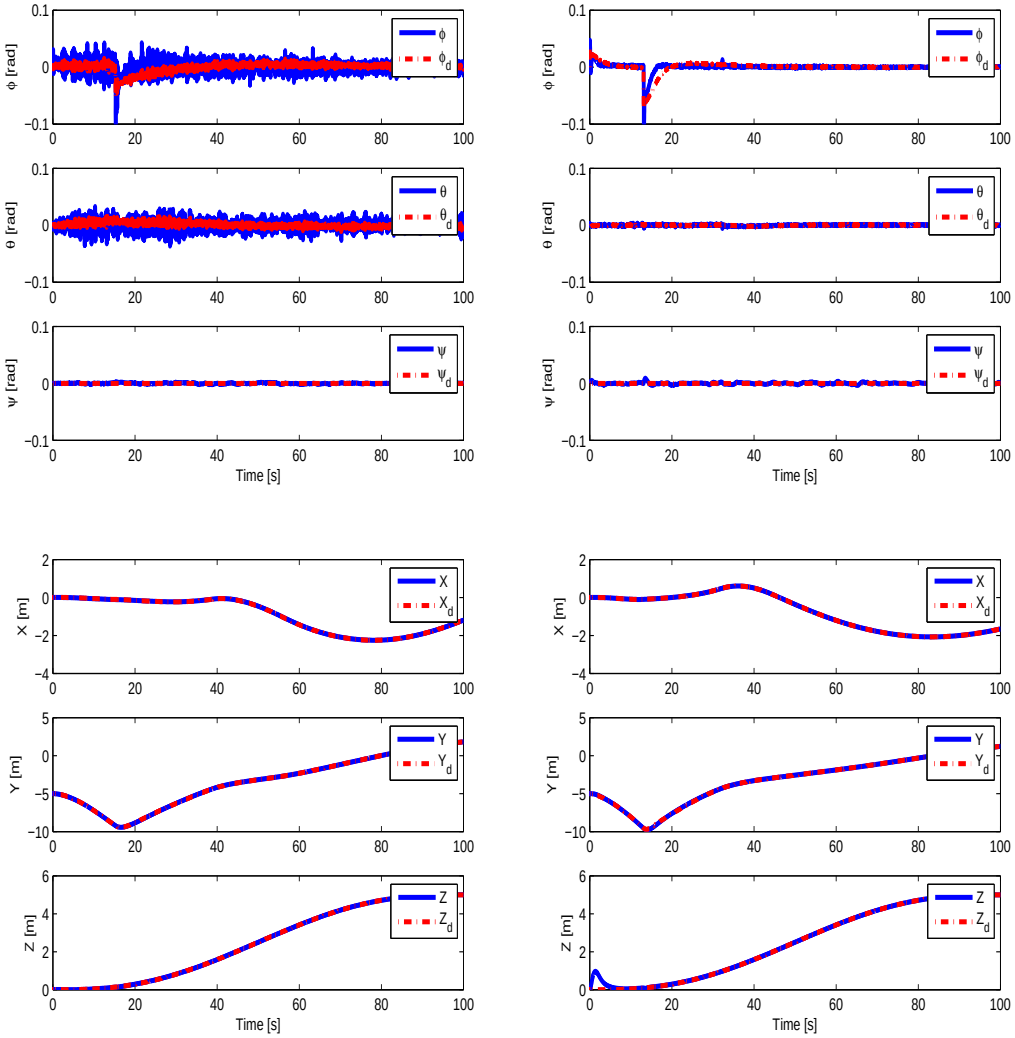

Figure 5.25: Attitude and Position tracking of the fifth quadrotor (Q_5) using (a) PID Control, (b) IB Control under external disturbance.

Table 5.6: RMS Errors for IB under External Disturbance Generated by Dryden Wind Model

Error	1. IB	2. IB	3. IB	4. IB	5. IB
e_ϕ (rad)	0.0010	0.0026	0.0025	0.0008	0.0056
e_θ (rad)	0.0026	0.0030	0.0006	0.0027	0.0007
e_ψ (rad)	0.0013	0.0012	0.0013	0.0014	0.0014
e_X (m)	0.0022	0.0027	0.0023	0.0045	0.0040
e_Y (m)	0.0019	0.0023	0.0017	0.0019	0.0110
e_Z (m)	0.1310	0.1310	0.1310	0.1311	0.1311

Table 5.7: RMS Errors for PID under External Disturbance Generated by Dryden Wind Model

Error	1. PID	2. PID	3. PID	4. PID	5. PID
e_ϕ (rad)	0.0069	0.0067	0.0063	0.0066	0.0099
e_θ (rad)	0.0074	0.0072	0.0062	0.0072	0.0084
e_ψ (rad)	0.0008	0.0007	0.0007	0.0007	0.0008
e_X (m)	0.0117	0.0132	0.0010	0.0123	0.0018
e_Y (m)	0.0030	0.0113	0.0116	0.0029	0.0292
e_Z (m)	0.0022	0.0020	0.0022	0.0022	0.0031

Chapter VI

6 Concluding Remarks and Future Works

In this thesis, coordination of a group of quadrotors is achieved by developing a reference model that consists of virtual springs and dampers that exert forces between the vehicles. In this system, a virtual plane is defined by orthogonally projecting quadrotor positions. On this virtual plane, planar distances between the quadrotors are utilized to exert virtual forces on each vehicle. Coordination among the quadrotors is achieved on a plane while altitude control is designed independently from this planar coordination.

In order to design flight controllers for individual quadrotors, the dynamics of the quadrotor is divided into two subsystems, namely position and attitude subsystems. Position and attitude controllers are designed by using integral backstepping control approach which is robust to the external disturbances such as wind. Reference attitude angles are computed by utilizing the dynamic inversion method and they are used by the attitude controllers.

Finally formation control problem of quadrotors is considered. The robots must be uniformly distributed on the final formation while they move in a coordinated fashion. Coordination and target forces are defined in terms of spring and damping forces where springs are adaptable. Spring coefficient is modeled as an adaptable parameter to reach the final formation around the target at a desired distance. Spring coefficient is switched after the first stage

of the coordinated task to enable achievement of the final formation. Sigmoid function is utilized for parameter switching problem to facilitate smoother response of the robots.

Simulation results provided for three and five quadrotors are quite promising. Quadrotors performed the coordinated tasks quite successfully. The number of robots can easily be increased, but simulation with 5 quadrotors show the potential of our method.

As a future work, we plan working on the physical implementation of the proposed coordination scheme. Once it is physically implemented, the coordinated motion of a group of unmanned aerial vehicle can be utilized for various coordinated tasks such as search, rescue, surveillance and border patrol by the aid of the proposed model in this thesis.

References

[1] Office of the Secretary of Defense. Unmanned Aerial Vehicles Roadmap 2005-2030, 2002.

[2] K. Nonami, F. Kendoul, S. Suzuki, W. Wang, and D. Nakazawa. *Autonomous Flying Robots : Unmanned Aerial Vehicles and Micro Aerial Vehicles*. Springer Verlag, Japan, 2010.

[3] Unmanned Aerial Vehicles Roadmap 2002-2027, December 2010.

[4] Robotics Trends, 2006. [online] `http://www.roboticstrends.com/displayarticle880.html`.

[5] Z. Sarris. Survey of UAV applicaitons in Civil Market. 2001.

[6] R. Finkelstein. The Ubiquitous UAV, 2009. [online] `http://www.robotictechnologyinc.com/images/upload/file/The_Ubiquitous_UAV.pdf`.

[7] U.S Army Unmanned Aircraft Systems Roadmap 2010-2035, 2010.

[8] Jorge Miguel Brito Domingues. Quadrotor prototype. Master's thesis, Universidade Tecnica de Lisboa, 2009.

[9] P. Castillo, R. Lozano, and A. Dzul. *Modelling and control of mini flying machines*. Springer Verlag, 2005.

[10] S. Grzonka, G. Grisetti, and W. Burgard. A fully autonomous indoor quadrotor. *Robotics, IEEE Transactions on*, 28(1):90–100, 2012.

[11] G.V. Raffo, M.G. Ortega, and F.R. Rubio. An integral predictive/nonlinear control structure for a quadrotor helicopter. *Automatica*, 46(1):29 – 39, 2010.

[12] S. Suzuki, R. Zhijia, Y. Horita, K. Nonami, G. Kimura, T. Bando, D. Hirabayashi, M. Furuya, and K. Yasuda. Attitude Control of Quad Rotors QTW-UAV with Tilt Wing Mechanism. *Journal of System Design and Dynamics*, 4:416–428, 2010.

[13] E. Cetinsoy, S. Dikyar, C. Hancer, K.T. Oner, E. Sirimoglu, M. Unel, and M.F. Aksit. Design and construction of a novel quad tilt-wing uav. *Mechatronics*, 22(6):723–745, Sept. 2012.

[14] Aerosonde Unmanned Aircraft System, June 2013. [online] `http://www.designation-systems.net/dusrm/app4/aerosonde.jpg`.

[15] Boeing X-45 B, June 2013. [online] `http://files.air-attack.com/MIL/_EXP/ucav/x45b.jpg`.

[16] Mikrocopter Quadrotor XL, June 2013. [online] `http://quadcopters.co.uk/ekmps/shops/quadcopters/images/mikrokopter-quadro-xl-kit-118-p.jpg`.

[17] Ascending Technologies Hummingbird Quadrotor, June 2013. [online] `http://www.asctec.de/uav-applications/research/products/asctec-hummingbird/`.

[18] QTW-UAS FS4, June 2013. [online] `http://www.barnardmicrosystems.com/Pictures/Tilt%20Wing%202%20QTW_4.jpg`.

[19] S. Bouabdallah, A. Noth, and R. Siegwart. Pid vs lq control techniques applied to an indoor micro quadrotor. In *Intelligent Robots and Systems, 2004. (IROS 2004). Proceedings. 2004 IEEE/RSJ International Conference on*, volume 3, pages 2451–2456 vol.3, 2004.

[20] H. Voos. Nonlinear control of a quadrotor micro-uav using feedback-linearization. In *Mechatronics, 2009. ICM 2009. IEEE International Conference on*, pages 1–6, 2009.

[21] E. Altug, J.P. Ostrowski, and R. Mahony. Control of a quadrotor helicopter using visual feedback. In *Robotics and Automation, 2002. Proceedings. ICRA '02. IEEE International Conference on*, pages 72–77, 2002.

[22] E. Altug, J.P. Ostrowski, and C.J. Taylor. Quadrotor control using dual camera visual feedback. In *Robotics and Automation, 2003. Proceedings. ICRA '03. IEEE International Conference on*, volume 3, pages 4294–4299 vol.3, 2003.

[23] S. Bouabdallah and R. Siegwart. Full control of a quadrotor. In *Intelligent Robots and Systems, 2007. IROS 2007. IEEE/RSJ International Conference on*, pages 153–158, 2007.

[24] C. Nicol, C.J.B. Macnab, and A. Ramirez-Serrano. Robust adaptive control of a quadrotor helicopter. *Mechatronics*, 21(6):927 – 938, 2011.

[25] R. Xu and U. Ozguner. Sliding mode control of a quadrotor helicopter. In *Decision and Control, 2006 45th IEEE Conference on*, pages 4957–4962, 2006.

[26] L. Luque-Vega, B. Castillo-Toledo, and Alexander G. Loukianov. Robust block second order sliding mode control for a quadrotor. *Journal of the Franklin Institute*, 349(2):719 – 739, 2012.

[27] H. Voos. Nonlinear and neural network-based control of a small four-rotor aerial robot. In *Advanced intelligent mechatronics, 2007 IEEE/ASME international conference on*, pages 1–6, 2007.

[28] G.M. Hoffmann, D.G. Rajnarayan, S.L. Waslander, D. Dostal, Jung Soon Jang, and C.J. Tomlin. The stanford testbed of autonomous rotorcraft for multi agent control (starmac). In *Digital Avionics Systems Conference, 2004. DASC 04. The 23rd*, volume 2, pages 12.E.4–121–10 Vol.2, 2004.

[29] S.L. Waslander, G.M. Hoffmann, Jung Soon Jang, and C.J. Tomlin. Multi-agent quadrotor testbed control design: integral sliding mode vs. reinforcement learning. In *Intelligent Robots and Systems, 2005. (IROS 2005). 2005 IEEE/RSJ International Conference on*, pages 3712–3717, 2005.

[30] J.H. Gillula, H. Huang, M.P. Vitus, and C.J. Tomlin. Design of guaranteed safe maneuvers using reachable sets: Autonomous quadrotor aerobatics in theory and practice. In *Robotics and Automation (ICRA), 2010 IEEE International Conference on*, pages 1649–1654, 2010.

[31] G.M. Hoffmann, H. Huang, S.L. Waslander, and C.J. Tomlin. Precision flight control for a multi-vehicle quadrotor helicopter testbed. *Control Engineering Practice*, 19(9):1023 – 1036, 2011.

[32] N. Michael, D. Mellinger, Q. Lindsey, and V. Kumar. The grasp multiple micro-uav testbed. *Robotics Automation Magazine, IEEE*, 17(3):56–65, 2010.

[33] N. Michael and V. Kumar. Control of ensembles of aerial robots. *Proceedings of the IEEE*, 99(9):1587–1602, 2011.

[34] A. Kushleyev, V. Kumar, and D. Mellinger. Towards a swarm of agile micro quadrotors. In *Proceedings of Robotics: Science and Systems*, Sydney, Australia, July 2012.

[35] M. Turpin, N. Michael, and V. Kumar. Trajectory design and control for aggressive formation flight with quadrotors. *Auton. Robots*, 33(1-2):143–156, August 2012.

[36] D. Mellinger, N. Michael, and V. Kumar. Trajectory generation and control for precise aggressive maneuvers with quadrotors. *I. J. Robotic Res.*, 31(5):664–674, 2012.

[37] M. Muller, S. Lupashin, and R. D'Andrea. Quadrocopter ball juggling. In *Intelligent Robots and Systems (IROS), 2011 IEEE/RSJ International Conference on*, pages 5113–5120, 2011.

[38] S. Lupashin, A. Schollig, M. Sherback, and R. D'Andrea. A simple learning strategy for high-speed quadrocopter multi-flips. In *Robotics and Automation (ICRA), 2010 IEEE International Conference on*, pages 1642–1648, 2010.

[39] M. Hehn and R. D'Andrea. A flying inverted pendulum. In *Robotics and Automation (ICRA), 2011 IEEE International Conference on*, pages 763–770, 2011.

[40] M.W. Mueller and R. D'Andrea. Critical subsystem failure mitigation in an indoor uav testbed. In *Intelligent Robots and Systems (IROS), 2012 IEEE/RSJ International Conference on*, pages 780–785, 2012.

[41] W. Ren and R.W. Beard. Virtual structure based spacecraft formation control with formation feedback. In *in AIAA Guidance, Navigation, and Control Conference, (Monterey, CA), American Institute of Aeronautics and Astronautics*, pages 2002–4963, 2002.

[42] W. Ren and R.W. Beard. Formation feedback control for multiple spacecraft via virtual structures. *Control Theory and Applications, IEE Proceedings* -, 151(3):357–368, 2004.

[43] R.C. Arkin. *An Behavior-based Robotics*. MIT Press, Cambridge, MA, USA, 1st edition, 1998.

[44] S. Monteiro and E. Bicho. A dynamical systems approach to behavior-based formation control. In *Robotics and Automation, 2002. Proceedings. ICRA '02. IEEE International Conference on*, volume 3, pages 2606–2611, 2002.

[45] B. Liu, R. Zhang, and C. Shi. Formation control of multiple behavior-based robots. In *Computational Intelligence and Security, 2006 International Conference on*, volume 1, pages 544–547, 2006.

[46] T. Soleymani and F. Saghafi. Behavior-based acceleration commanded formation flight control. In *Control Automation and Systems (ICCAS), 2010 International Conference on*, pages 1340–1345, 2010.

[47] M. Xiaomin, D. Yang, L. Xing, and W. Sentang. Behavior-based formation control of multi-missiles. In *Control and Decision Conference, 2009. CCDC '09. Chinese*, pages 5019–5023, 2009.

[48] Q. Jia and G. Li. Formation control and obstacle avoidance algorithm of multiple autonomous underwater vehicles(auvs) based on potential function and behavior rules. In *Automation and Logistics, 2007 IEEE International Conference on*, pages 569–573, 2007.

[49] F. Arrichiello, S. Chiaverini, and T.I. Fossen. Formation control of marine surface vessels using the null-space-based behavioral control. In K.Y Pettersen, J.T Gravdahl, and H. Nijmeijer, editors, *Group Coordination and Cooperative Control*, volume 336 of *Lecture Notes in Control and Information Science*, pages 1–19. Springer Berlin Heidelberg, 2006.

[50] G. Quintana-Carapia, J.S. Benitez-Read, and J.A. Segovia-De-Los-Rios. Null space based behavior control applied to robot formation. In *World Automation Congress (WAC), 2012*, pages 1–6, 2012.

[51] A. Davidi, N. Berman, and S. Arogeti. Formation flight using multiple integral backstepping controllers. In *Cybernetics and Intelligent Systems (CIS), 2011 IEEE 5th International Conference on*, pages 317–322, 2011.

[52] H. Sira-Ramirez and R. Castro-Linares. Trajectory tracking for nonholonomic cars: A linear approach to controlled leader-follower formation. In *Decision and Control (CDC), 2010 49th IEEE Conference on*, pages 546–551, 2010.

[53] J. Ghommam, H. Mehrjerdi, and M. Saad. Leader-follower formation control of nonholonomic robots with fuzzy logic based approach for obstacle avoidance. In *Intelligent Robots and Systems (IROS), 2011 IEEE/RSJ International Conference on*, pages 2340–2345, 2011.

[54] J. Guo, Z. Lin, M. Cao, and G. Yan. Adaptive leader-follower formation control for autonomous mobile robots. In *American Control Conference (ACC), 2010*, pages 6822–6827, 2010.

[55] L. Consolini, F. Morbidi, D. Prattichizzo, and M. Tosques. On the control of a leader-follower formation of nonholonomic mobile robots. In *Decision and Control, 2006 45th IEEE Conference on*, pages 5992–5997, 2006.

[56] A.P. Dani, N. Gans, and W.E. Dixon. Position-based visual servo control of leader-follower formation using image-based relative pose and relative velocity estimation. In *American Control Conference, 2009. ACC '09.*, pages 5271–5276, 2009.

[57] R. Cui, S. Sam Ge, B. Voon Ee How, and Yoo Sang Choo. Leader-follower formation control of underactuated auvs with leader position measurement. In *Robotics and Automation, 2009. ICRA '09. IEEE International Conference on*, pages 979–984, 2009.

[58] X. Chen, A. Serrani, and H. Ozbay. Control of leader-follower formations of terrestrial uavs. In *Decision and Control, 2003. Proceedings. 42nd IEEE Conference on*, volume 1, pages 498–503 Vol.1, 2003.

[59] T. Dierks and S. Jagannathan. Neural network control of quadrotor uav

formations. In *American Control Conference, 2009. ACC '09.*, pages 2990–2996, 2009.

[60] W. Ren and R.W. Beard. A decentralized scheme for spacecraft formation flying via the virtual structure approach. In *American Control Conference, 2003. Proceedings of the 2003*, volume 2, pages 1746–1751, 2003.

[61] J. Yuan and G.Y. Tang. Formation control for mobile multiple robots based on hierarchical virtual structures. In *Control and Automation (ICCA), 2010 8th IEEE International Conference on*, pages 393–398, 2010.

[62] P. Urcola, L. Riazuelo, M.T. Lazaro, and L. Montano. Cooperative navigation using environment compliant robot formations. In *Intelligent Robots and Systems, 2008. IROS 2008. IEEE/RSJ International Conference on*, pages 2789–2794, 2008.

[63] T.H.A Van den Broek, N. Van de Wouw, and H. Nijmeijer. Formation control of unicycle mobile robots: a virtual structure approach. In *Decision and Control, 2009 held jointly with the 2009 28th Chinese Control Conference. CDC/CCC 2009. Proceedings of the 48th IEEE Conference on*, pages 8328–8333, 2009.

[64] E. Lalish, K.A. Morgansen, and T. Tsukamaki. Formation tracking control using virtual structures and deconfliction. In *Decision and Control, 2006 45th IEEE Conference on*, pages 5699–5705, 2006.

[65] N.H.M. Linorman and H.H.T. Liu. Formation uav flight control us-

ing virtual structure and motion synchronization. In *American Control Conference, 2008*, pages 1782–1787, 2008.

[66] C.B. Low. A dynamic virtual structure formation control for fixed-wing uavs. In *Control and Automation (ICCA), 2011 9th IEEE International Conference on*, pages 627–632, 2011.

[67] C.B. Low and Q. San Ng. A flexible virtual structure formation keeping control for fixed-wing uavs. In *Control and Automation (ICCA), 2011 9th IEEE International Conference on*, pages 621–626, 2011.

[68] Laura Krick. Application of Graph Rigidity in Formation Control of Multi-Robot Networks. Master's thesis, University of Toronto, 2007.

[69] W.J. Dong, Yi Guo, and J.A. Farrell. Formation control of nonholonomic mobile robots. In *American Control Conference, 2006*, pages 6 pp.–, 2006.

[70] W. Dong and J.A. Farrell. Cooperative control of multiple nonholonomic mobile agents. *Automatic Control, IEEE Transactions on*, 53(6):1434–1448, 2008.

[71] J.A. Fax and R.M. Murray. Information flow and cooperative control of vehicle formations. *Automatic Control, IEEE Transactions on*, 49(9):1465–1476, 2004.

[72] T. Azuma and T. Karube. Formation control with fault-tolerance based on rigid graph theory. In *SICE Annual Conference 2010, Proceedings of*, pages 1137–1140, 2010.

[73] J.C. Derenick, J.R Spletzer, and M.A Hsieh. A graph theoretic approach to optimal target tracking for mobile robot teams. In *Intelligent Robots and Systems, 2007. IROS 2007. IEEE/RSJ International Conference on*, pages 3422–3428, 2007.

[74] M.M. Zavlanos, M.B Egerstedt, and G.J. Pappas. Graph-theoretic connectivity control of mobile robot networks. *Proceedings of the IEEE*, 99(9):1525–1540, 2011.

[75] M.C. De Gennaro and A. Jadbabaie. Decentralized control of connectivity for multi-agent systems. In *Decision and Control, 2006 45th IEEE Conference on*, pages 3628–3633, 2006.

[76] J. Barca, A. Sekercioglu, and A. Ford. Controlling formations of robots with graph theory. In S. Lee, H. Cho, K.J Yoon, and J. Lee, editors, *Intelligent Autonomous Systems 12*, volume 194 of *Advances in Intelligent Systems and Computing*, pages 563–574. Springer Berlin Heidelberg, 2013.

[77] Nusrettin Gulec. Modeling and control of the coordinated motion of a group of autonomous mobile robots. Master's thesis, Sabanci University, 2005.

[78] N. Gulec and M. Unel. A novel coordination scheme applied to nonholonomic mobile robots. In *Decision and Control, 2005 and 2005 European Control Conference. CDC-ECC '05. 44th IEEE Conference on*, pages 5089–5094, 2005.

[79] Steven L. Waslander and Carlos Wang. Wind disturbance estimation and rejection for quadrotor position control. *In AIAA In-*

fotech@Aerospace Conference and AIAA Unmanned...Unlimited Conference, April 2009.